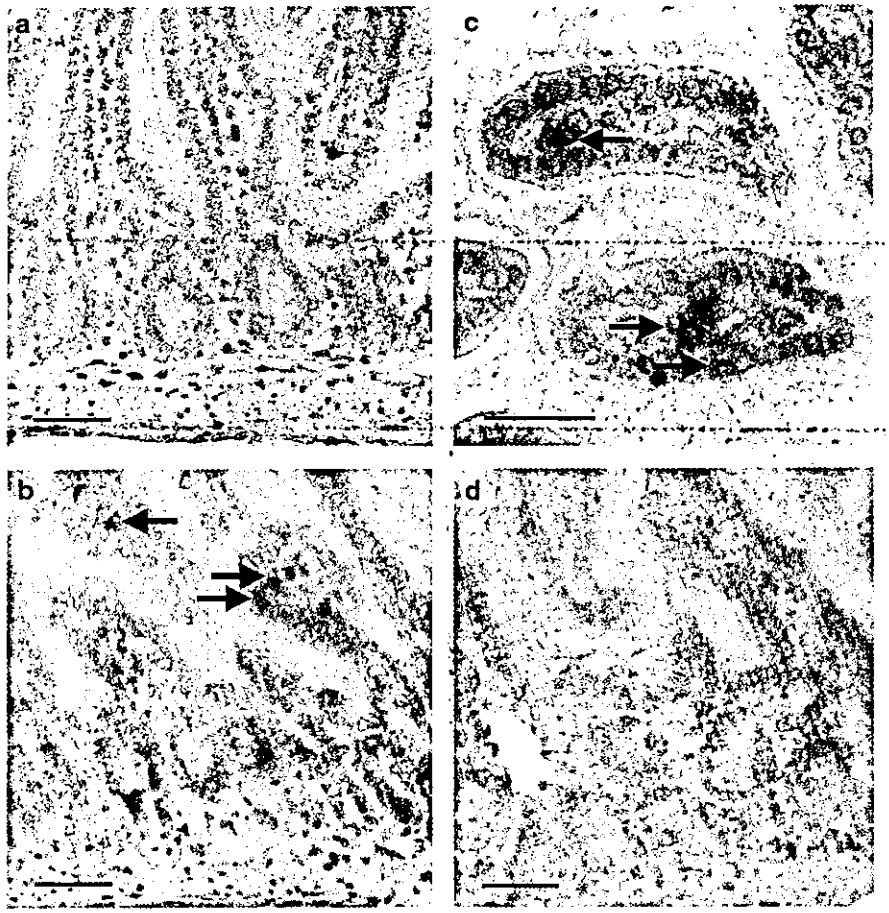

Figure 4 Immunostaining of serial sections of small intestine tissue from mice 2 days after oral administration of pJWNL432-encapsulated VLPs. HIV env proteins were observed in epithelial cells (arrow) (b, c), and control mAb did not show any positive reactions (d). Control mice were also administered pJWNL432 without VLP encapsulation (a). Bar marker represents 50 μm.

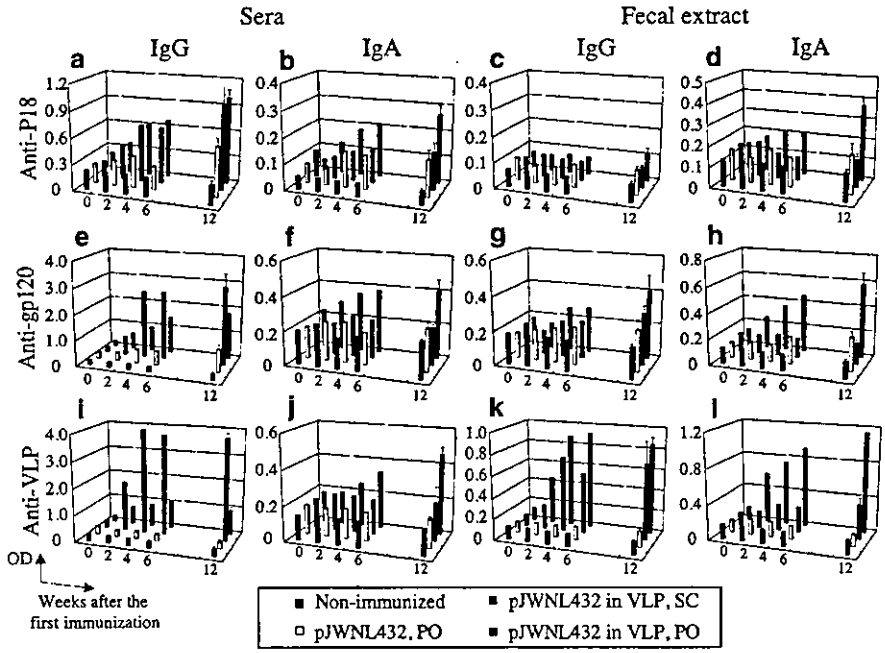

Figure 5 IgG (a, c, e ,g, i and k) and IgA (b, d, f, h, j and l) levels in sera (a, b, e, f, i and j) and fecal extracts (c, d, g, h, k and l) of immunized mice. Mice were orally (■) or subcutaneously (□) administered pJWNL432 encapsulated in VLP or naked (■). Symbols indicate HIV env-specific antibody levels. Background levels to HIV env in nonimmunized mice (■) are also shown. The IgG and IgA antibody levels are expressed as OD at dilutions of 1:100 and 1:2 for serum and fecal extracts, respectively. The mean OD values ±s.e.s were obtained from five mice/group.

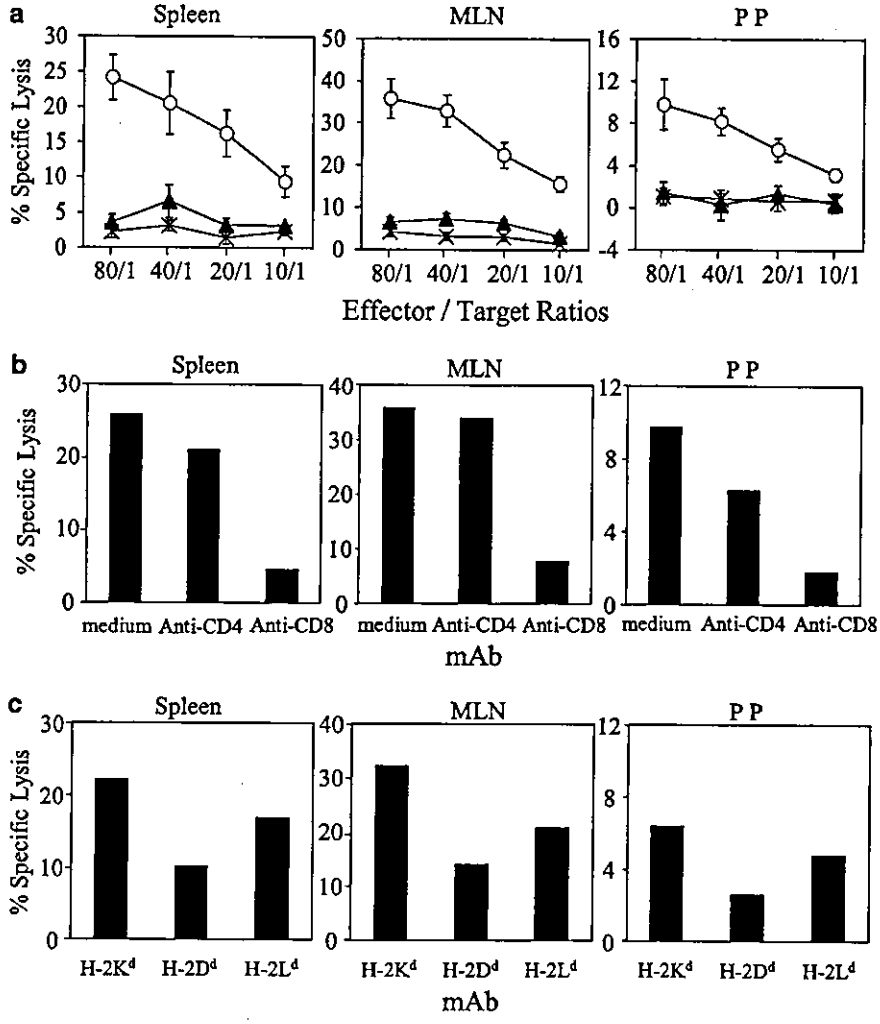

Figure 6 Spleen, MLN and PP cells from mice orally administered pJWNL432-encapsulated VLPs elicited CTL. (a) Mice were orally administered pJWNL432 encapsulated in VLPs (circles) or naked (triangles). Results for nonimmunized controls are also shown (×). (b) Effector cells obtained from the spleen, MLN and PP cells of mice orally administered pJWNL432-encapsulated VLPs are mediated CD8+ cells. Lytic activities of effector cells were assessed in the presence of anti CD4 mAb, anti-CD8 mAb or medium. Effector:target ratio was 80:1. (c) HIV env-specific lysis was restricted by MHC class I. Effector cells were examined for P18-specific lytic activities in the presence of anti-H-2K^d, anti-H-2D^d or H-2L^d mAb. The percentage of P18-specific lysis was calculated as (% lysis of target cells labeled with P18)−(% lysis of target cells labeled with control peptide). Each value is the mean percentage of the specific lysis values obtained from five mice.

pathogens is mucosal vaccines that are capable of inducing both systemic and mucosal immunity. Recent evidence has shown that DNA vaccination can confer protection against a number of infectious agents, including viruses and bacteria, although peripheral immunization with naked DNA is less than optimal for stimulating mucosal immunity.[12,13] In fact, it is quite difficult to induce both mucosal and systemic immune responses by oral administration of naked DNA. This study demonstrated that an orally administered DNA vaccine encapsulated in an orally transmissible virus-derived VLP induced both mucosal and systemic immunity.

The delivery of a DNA vaccine for induction of mucosal immune responses is usually achieved by gene transfer to the upper nasopharynx-associated lymphoid tissue (NALT), upper airway, salivary glands, and tonsils.[5,14] Despite its obvious convenience, oral administration is rarely successful, since it is quite difficult to protect plasmid DNA from the environment in the digestive tract. The efficacy of orally delivered DNA vaccine to NALT is improved by encapsulating plasmid DNA in poly (lactide-coglycolide) (PLG) microparticles for protection against the gastric environment.[15,16] The immune responses to particle-borne DNA immunizations by means such as utilization of a gene gun or PLG differ from those to DNA immunizations without particles.[13] It is thought that the microparticles are actively taken up by cells such as macrophages or M cells of PP of the small intestine and thus facilitate the presentation of antigens to local immune systems.[15,17] This mechanism is the same as that of gene gun immunization of a DNA vaccine, that is, phagocytic cells such as macrophages or dendritic cells take up plasmid DNA delivered by a gene gun. The delivered gene is expressed only in these cells.[18] Similarly, only mucosal immunity was induced in mice by oral administration of DNA-encapsulated PLG microparticles.[15,16] It is likely that the mechanism underlying immune recognition of

HEV-VLP infection is similar to that of direct intramuscular or subcutaneous DNA immunization without the use of particles. Protein expressed by HEV-VLP-infected cells is recognized by the immune surveillance system, resulting in the elicitation of Ag-specific immune responses. We showed in this study that genes could be expressed in epithelial cells in the small intestine after delivery by HEV-VLPs (Figure 4). It is plausible that HEV-VLPs, which are derived from an orally transmissible virus, were incorporated into HEV-permissive epithelial cells in the small intestine, because they retained structures and properties similar to those of HEV particles, producing an infection similar to that induced naturally.[19] The Ag-expressing cells might be recognized by intraepithelial lymphocytes or submucous antigen-presenting cells by the same mechanism as that in the case of general virus infection.

An HEV-VLP has several advantages as a vector of DNA. Firstly, in our experience, large amounts can be easily obtained from standard cultivation protocols compared with the amounts of other VLPs obtained. The yield of purified HEV-VLPs collected from a culture supernatant of 50–100 μg/ml is more than 100 times greater than that of other VLPs. Secondly, the outcome of gene delivery in humans can be predicted using conventional laboratory animals, since HEV naturally infects various animals as well as humans through the same infectious route and target cells.[10,20] Thirdly, HEV-VLPs are stable at room temperature. Fourthly, anti-HEV immune responses had no effect on DNA administration in the present study, and this might be related to the neutralizing antibody for preventing infection with HEV. Neutralizing antibodies to HEV for inhibiting infection have not yet been found. This is also the case for HCV. The mechanism by which HEV is eliminated by antibodies is thought to be antibody-dependent cell-mediated cytotoxicity (ADCC). The effect of induction of immune responses to DNA vaccine in our system is not clear. Thus, HEV-VLPs are an attractive vaccine vector in developing countries because these VLP can be preserved without the requirement of any particular equipment. Finally, we have reported that an HEV-VLP can carry foreign amino-acid sequences as a part of the ORF2 protein exposed on the particle surface without any morphological or biological alteration.[10] Liposomal vectors resembling retroviral envelopes endowed with targeting molecules for gene delivery have been reported. The vicronectin receptor, $\alpha_v\beta_3$-integrin, is commonly upregulated on malignant melanoma cells, and liposome carrying an Arg-Gly-Asp (RGD) integrin-binding motif has been used for a system to deliver DNA to these tumor cells.[21] It has also been reported that targeting DNA to M cells by intranasal administration for the induction of mucosal and systemic responses can be achieved by formulating DNA with polylysine linked to viral adhesion.[22] It may be possible to design chimeric ORF2 proteins carrying these targeting molecules to retarget HEV-VLP to particular cell types.

Oral vaccination has obvious advantages for a field trial in a large-scale public health vaccination program.[23] From a practical standpoint, oral administration is less stressful for vaccine recipients and does not require professional skill for the vaccine administration. Moreover, delivery of vaccines via the intestinal tract is considered to be inherently safer than systemic injection. Encouraging results of phase I trials using Norwalk virus VLPs have recently been reported.[24] Trials using DNA vaccines for infectious and malignancy diseases have also been conducted.[25] The results of the present study suggest that oral administration of DNA vaccine encapsulated in oral transmissible virus VLPs, HEV-VLPs, is effective for inducing both humoral and cellular immunity locally as well as systematically. HEV-VLPs might be useful not only for vaccination but also as a vector in human gene therapy.

Materials and methods

Mice

BALB/c female mice were purchased from Clea Japan (Tokyo, Japan) and were housed in the Laboratory Animal Center of Mie University School of Medicine during the experimental period.

Peptide synthesis

The peptides used in this study were the HIV env CTL epitope (HIV 308-322, RIQRGPGRAFVTIGK; P18)[26] and a control peptide (HCV nonstructural protein 5 CTL epitope MSYSWTGALVTPCAAE; P17).[27]

Plasmid DNA

A highly efficient mammalian expression vector, pJW4303,[28] was used for efficient expression of HIV env gp120 of the NL432 strain.[29] Various sizes of plasmid DNA were also used for the *in vitro* packaging experiment (3.162 kb: pUC118; 5.93 kb: pJW322; 8.63 kb: pJWSIVenv; 11.2 kb: pABWN).

Production and purification of HEV-VLPs

HEV-VLPs were produced and purified by previously described methods.[10,11] Briefly, Tn5 cells maintained in Excel 405 serum-free medium (JRH, KS) were infected with the recombinant baculovirus expressing HEV-ORF2 at an m.o.i. of >5 and cultured for 6 days. The supernatant was harvested and the recombinant baculovirus in the supernatant was pelleted by ultracentrifugation at 10 000 *g* for 30 min at 4°C. The VLPs in the supernatant were collected by further ultracentrifugation at 100 000 *g* for 2 h at 4°C. Pelleted VLPs were then resuspended in 10 mM potassium-[2-(*N*-morpholino) ethanesulfonic acid] (MES) buffer (pH 6.2) and purified on a CsCl equilibrium density gradient. The purified HEV-VLPs were spun down and resuspended in potassium-MES buffer and kept at 4°C.

DNA packaging

Plasmid DNA was encapsulated into HEV-VLPs according to a previously described procedure.[30] Purified VLPs (50 μg) were disrupted by incubation in 180 μl of a buffer containing 50 mM Tris-HCl (pH 7.5), 150 mM NaCl, 1 mM EGTA and 20 mM dithiothreitol. Following 30 min of incubation at room temperature, 200 μg (20 μl) of each plasmid in 50 mM Tris-HCl buffer (pH 7.5) and 150 mM NaCl was added. The disrupted VLP preparation was refolded by incubation for 1 h with increasing concentrations of $CaCl_2$ up to a final concentration of 5 mM. VLPs were pelleted by ultracentrifugation and resuspended in 10 mM potassium-MES buffer (pH 6.2). At each step, the VLP structure formation was confirmed by electron

microscopy after negative staining, as described previously.[11] To estimate the amounts of encapsulated plasmid DNA, refolded and purified VLPs were treated with 10 IU benzonase (SIGMA-ALDRICH, Irvin, UK) for 1 h at 20°C to remove DNA on the surfaces of VLPs and disrupted with EGTA (1 mM). Absorbance of the supernatant was measured for detection of plasmid DNA contents.

Density analysis of refolded VLPs

Refolded VLPs were separated on a CsCl equilibrium density gradient and fractioned into 0.2 ml aliquots. HEV-VLPs in each fraction were detected by ELISA as previously described,[10] as well as DNA contents.

Gene transfer in mammalian cells

Four cell lines (NIH/3T3 (mouse), RK13 (rabbit), COS-7 (monkey), HepG2 (human)) were used in transfection experiments. Sterilized coverslips were placed in six-well plates, and 5×10^5 cells per well were seeded in the plates. After overnight culture, cells were washed twice with a medium, and about 1 μg of VLP-encapsulated EGFP expression vector (BD Bioscience Clontech, CA, USA) diluted with 0.5 ml medium was added. After 2 h of incubation at 37°C, VLPs were removed. Cells were then incubated for 48 h at 37°C. At the end of the culture period, cells were removed from the culture medium and washed three times with PBS. Coverslips were then mounted onto microscope slide glasses. Fluorescence of the GFP-expressing cells was observed under a fluorescence microscope.

Immunization

Mice were orally immunized four times with 50 μg protein of HEV-VLP/DNA (pJWNL432) complex or 20 μg naked pJWNL432 DNA in 100 μl of potassium-MES buffer at 1 week intervals.

Immunohistochemical analysis

At 2 days after oral immunization, the mice were killed and tissues were collected. Cryostat sections were air-dried and incubated in 0.5% HIO_4 for 10 min to quench endogenous peroxidase activity. The sections were further pretreated with chicken anti-mouse IgG antibody (Chemicon International, Inc., CA, USA) to prevent nonspecific reactions of a secondary antibody. The sections were then incubated with an HIV env-specific mAb (HIV-1 IIIB gp120 mAb (902)), which was obtained through the AIDS Research and Reference Reagent Program,[31] for 30 min at 37°C. The bound antibodies were visualized with a biotinated secondary antibody, HRP-labeled avidin–biotin complex (ABC-peroxidase staining kit, Elite Vector Lab. Inc., CA, USA) and 3.3′-diaminobenzidine tetrachloride with 0.01% H_2O_2. Sections were slightly counterstained with hematoxylin. An mAb (A1/3D1, ANOGEN, Canada) against hepatitis C virus core, which is same isotype to 902, was used as a control.

ELISA

Serum and fecal samples were collected at 0 (preimmunization), 2, 4, 6 and 12 weeks after the first immunization. Feces were suspended in ice-cold PBS at 200 mg/ml, and the centrifuge supernatant was used as fecal extract. Culture plates (96-well) were coated with purified HEV-VLPs or synthesized oligopeptides (P18) at a concentration of 10 or 100 μg/well, respectively, overnight at 4°C followed by 30 min of blocking with PBS containing 0.1% FBS and 0.05% Tween 20. To determine the anti-HIV env gp120 antibody responses, CV-1 cells were seeded in 96-well plates and infected with recombinant Sendai virus expressing HIV env gp120 of NL432 strain (SeV gp120),[32] and then the plates were incubated at 37°C. At 3 days after infection, plates were washed and fixed with PBS containing 10% formalin for 10 min. Test samples were added to each well and incubated at room temperature for 1 h. For detection of anti-HIV env gp120 antibody, test samples were reacted with wild-type Sendai virus-infected CV-1 cells before addition to the wells to eliminate the nonspecific antibody. Biotin-labeled anti-mouse IgG (Vector, CA, USA) or IgA (CALTAG, CA, USA) was used as the detection antibody. Following 1 h incubation, the plates were washed and further incubated with avidin-HRP (Vector, CA, USA). The reaction was developed using an ABTS substrate (Roch Diagnostic, Mannheim, Germany).

Generation of CTL effector cells

Effector cells were derived from spleen, MLN and PP cells as precursor CTLs. Aliquots of 5×10^6 spleen cells were co-cultured with 2.5×10^6 mitomycin C-treated autologous spleen cells labeled with a peptide at 37°C in a CO_2 incubator. The effector cells generated were harvested after 5 days of culture.

Cytotoxicity assay

Target cells, A20.2J cells (2×10^6), were incubated at 37°C in a 5% CO_2 atmosphere with 10 μg/ml of P18 or control peptide for 16 h. The target cells were then washed and labeled with ^{51}Cr. The ^{51}Cr-labeled target cells were incubated for 5 h with effector cells. Spontaneous release varied from 5 to 10%. Percent lysis was calculated as ((experimental release−spontaneous release)/(100% release−spontaneous release)) × 100. All the experiments were performed at least four times, and each experimental group consisted of five mice.

Blocking of cytolysis

^{51}Cr-labeled target cells (10^6 cells) were preincubated at 4°C for 1 h with anti-H-2 K^d, D^d or L^d mAb (Meiji Institute of Health Science Ltd., Tokyo, Japan) (1 μg/ml), and effector cells were then added. In a separate experiment, effector cells (10^7 cells) were preincubated with anti-CD4 mAb (GK1.5) or anti-CD8 mAb (Lyt2.2) (10 μg/ml) at 4°C for 1 h, and then the labeled target cells were added. Blocking of cytolytic activities by these mAbs was assessed by a 5-h ^{51}Cr release assay.

Statistical analysis

Statistical analysis was performed using Mann–Whitney's U test and Kruskal–Wallis test. Values are expressed as means±s.d.s. A 95% confidence limit was taken as significant ($P<0.05$).

Acknowledgements

This work was supported by Health Science Research Grants from the Ministry of Health, Labor and Welfare of Japan and the Ministry of Education, Culture, Sports, Science and Technology of Japan.

References

1 Hoffmann C *et al*. Efficient gene transfer into human hepatocytes by baculovirus vectors. *Proc Natl Acad Sci USA* 1995; **92**: 10099–10103.
2 Mistry AR *et al*. Recombinant HMG1 protein produced in *Pichia pastoris*: a nonviral gene delivery agent. *Biotechniques* 1997; **22**: 718–729.
3 Schneider H *et al*. Gene transfer mediated by alpha2-macroglobulin. *Nucleic Acids Res* 1996; **24**: 3873–3874.
4 Afione A, Conrad CK, Flotte TR. Gene therapy vectors as drug delivery systems. *Clin Pharmacokinet* 1995; **28**: 181–189.
5 Morrow CD *et al*. Recombinant viruses as vectors for mucosal immunity. In: Kraehenbuhl JP, Neutra MR (eds). *Defense of Mucosal Surfaces: Pathiogenesis, Immunity and Vaccines. Current Topics in Microbiology and Immunology*, Vol. 236 Springer-Verlag: Berlin, 1999, pp 255–273.
6 Ogra PL, Faden H, Welliver RC. Vaccination strategies for mucosal immune responses. *Clin Microbiol Rev* 2001; **14**: 430–435.
7 Medina E, Guzman CA. Modulation of immune responses following antigen administration by mucosal route. *FEMS Immunol Med Microbiol* 2000; **27**: 305–311.
8 Ulrich R, Nassal M, Meisel H, Kruger DH. Core particles of hepatitis B virus as carrier for foreign epitopes. *Adv Virus Res* 1998; **50**: 141–182.
9 Clark B *et al*. Immunity against both polyomavirus VP1 and a transgene product following intranasal delivery of VP1 pseudocapsid–DNA complexes. *J Gen Virol* 2001; **82**: 2791–2797.
10 Li TC *et al*. Expression and self-assembly of empty virus-like particles of hepatitis E virus. *J Virol* 1997; **71**: 7207–7213.
11 Niikura M *et al*. Chimeric recombinant hepatitis E virus-like particles as an oral vaccine vehicle presenting foreign epitopes. *Virology* 2002; **293**: 273–280.
12 Etchart N *et al*. Class-I restricted CTL induction by mucosal immunization with naked DNA encoding measles virus haemagglutinin. *J Gen Virol* 1997; **78**: 1577–1580.
13 Feltquate DM, Heaney S, Webster RG, Robinson HL. Different T helper cell types and antibody isotypes generated by saline and gene gun DNA immunization. *J Immunol* 1997; **158**: 2278–2284.
14 McCluskie MJ *et al*. Direct gene transfer to the respiratory tract of mice with pure plasmid and lipid formulated DNA. *Antisense Nucleic Acid Drug Dev* 1998; **8**: 401–414.
15 Kaneko H *et al*. Oral DNA vaccination promotes mucosal and systemic immune responses to HIV envelope glycoprotein. *Virology* 2000; **267**: 8–16.
16 Chen SC *et al*. Protective immunity induced by oral immunization with a rotavirus DNA vaccine encapsulated in microparticles. *J Virol* 1998; **72**: 5757–5761.
17 Eldridge JH *et al*. Controlled vaccine release in the gut-associated lymphoid tissues. I. Orally administered biodegradable microspheres target the Payer's patches. *J Control Rel* 1990; **11**: 205–214.
18 Condon C *et al*. DNA-based immunization by *in vivo* transfection of dendriric cells. *Nat Med* 1996; **10**: 1122–1128.
19 Li TC *et al*. Oral administration of hepatitis E virus-like particles induces a systemic and mucosal immune response in mice. *Vaccine* 2001; **14**: 3476–3484.
20 Worm HC, van der Poel WHM, Brandstartter G. Hepatitis E: an overview. *Microbes Inf* 2002; **4**: 657–666.
21 Nahde T *et al*. Combined transductional and transcriptional targeting of melanoma cerlls by artificial virus-like particles. *J Gene Med* 2001; **3**: 353–361.
22 Wu Y *et al*. M cell-targeted DNA vaccination. *Proc Natl Acad Sci USA* 2001; **98**: 9318–9323.
23 Nagaraj K, Babu BV. Field trials of oral cholera vaccine in Vietnam. *Lancet* 1997; **349**: 1253–1254.
24 Ball JM *et al*. Recombinant Norwalk virus-like particles given orally to volunteers: phase 1 study. *Gastroenterology* 1999; **117**: 40–48.
25 Promoting the free-flow of information within the DNA vaccine community URL: http://dnavaccine.com.
26 Takahashi H *et al*. An immunodominant epitope of the human immunodeficiency virus envelope glycoprotein gp160 recognized by class I major histocompatibility complex molecule-restricted murine cytotoxic T lymphocytes. *Proc Natl Acad Sci USA* 1988; **85**: 3105–3109.
27 Shirai M *et al*. Induction of cytotoxic T cells a cross-reactive epitope in the hepatitis C virus nonstructural RNA polymerase-like protein. *J Virol* 1992; **66**: 4908–4106.
28 Yasutomi Y *et al*. Simian immunodeficiency virus-specific cytotoxic T lymphocyte induction through DNA vaccination of rhesus monkeys. *J Virol* 1996; **70**: 678–681.
29 Adachi A *et al*. Production of acquired immunodeficiency syndrome-associated retrovirus in human and nonhuman cells transfected with an infectious molecular clone. *J Virol* 1986; **59**: 284–291.
30 Touze A, Coursaget P. *In vitro* gene transfer using human papillomavirus-like particles. *Nucleic Acids Res* 1998; **26**: 1317–1323.
31 Picnus SH, Wehrly K, Chesebro B. Treatment of HIV tissue culture infection with monoclonal antibody–ricin A chain conjugate. *J Immunol* 1998; **142**: 3070–3075.
32 Toriyoshi H *et al*. Sendai virus-based production of HIV type 1 subtype B and subtype E envelope glycoprotein 120 antigens and their use for highly sensitive detection of subtype-specific serum antibodies. *AIDS Res Hum Retroviruses* 1999; **15**: 1109–1120.

■ ワクチン

ウイルス様中空粒子(VLP)を用いた経口ワクチン

保富康宏 三重大学医学部 生体防御医学講座

〔論文要旨〕
近年SARSや鳥インフルエンザのヒトへの感染など感染症の危機は年々つのってきている．また感染症は先進国で制圧，コントロールされても発展途上国で長期にわたり存在し，世界的に安全と考えられるには長い時間が必要となる．この様な中でワクチン開発は感染症の危険を取り除くのに必須の手段となる．本文ではウイルス様中空粒子(VLP)を用いた新たな手法のワクチンの可能性について述べる[1,2]．

1. 経口ワクチンの必要性

多くの感染症が呼吸器や消化器，生殖器等の粘膜を介し感染を成立させていることは周知である．そのために粘膜面に特異免疫を誘導し，感染症をコントロールすることは理にかなっている．しかしながら粘膜免疫の特徴上通常のワクチン抗原の皮下接種等では全身性の免疫の誘導は可能であるが，粘膜免疫の誘導は困難である．粘膜免疫では一部の粘膜で誘導された免疫反応が連続していなくても多くの粘膜面や分泌腺で同時に誘導されると考えられている[3]．このため，粘膜面に有効にワクチン抗原を運ぶことが出来れば粘膜ワクチンが可能となる．

経口的にワクチン抗原を投与し消化器粘膜から免疫反応を誘導することは呼吸器等の粘膜面に抗原を投与し，免疫反応を誘導すること以上に困難である．極端に低いpH，消化酵素等の存在が抗原を安定して消化管内に存在させることを困難にしている原因である．しかしながら多くの細菌やウイルスが消化器系に感染することを考えれば，それらを利用すれば可能ではないかと考えられる．実際，消化器粘膜から感染を示す細菌を用いて遺伝子組み込んだワクチンの報告がなされている．著者自身も遺伝子組み込みBCGの報告をしているが，この抗酸菌BCGも消化器から免疫反応を誘導することが可能である[4,5]．

経口ワクチンの利点は特別な手技，技術，道具等を必要としないこと，それにより大きな規模のフィールドトライアルが行えることである．更にワクチンを受ける側にもストレスを与えないために幼児にも負担が少なく投与できる．経口的に投与できるという利点を考えると人獣共通伝染病への利用は比較的早期に行える可能性がある．家畜等では管理者によりワクチン接種が可能ではあるが，野生動物が保持しヒトへの感染の危険性を持つもの，狂犬病や日本脳炎，E型肝炎ウイルス等には餌に混入させ散布する方法もある．実際野生動物に対し狂犬病ワクチン混入の餌の散布を試みている国も存在する[6-8]．経口ワクチンの利点として加えるならば，その安全性も一つであろう．生体の持つ防御反応では極めて大きな役割を持つ嘔吐や排泄がこれにあたる．この様に経口ワクチンはその魅力と困難さの両者を併せ持っている．以下に著者らが行っているE型肝炎ウイルス(HEV)のウイルス様中空粒子(VLP)を用いた経口ワクチンの試みについて述べる．

Oral administration of vaccine by using virus-like particle
Yasuhiro YASUTOMI, Department of Bioregulation, Mie University School of Medicine
別刷請求先：保富康宏 〒514-8507 三重県津市江戸橋2-174 三重大学医学部生体防御医学講座
Tel：0590-231-5410 Fax：059-231-5410 e-mail：yasutomi@doc.medic.mie-u.ac.jp

2. E型肝炎ウイルス(HEV)

HEVはカリシウイルス科に類似している一本鎖＋鎖RNAウイルスである．当初東南アジアを中心に流行性に発生していたが，A型肝炎ウイルスの測定が可能となった結果HAVと異なるウイルスであることが判明し，1980年代末に新しい肝炎ウイルスであることがわかった．HEVは経口的に小腸粘膜より感染し，門脈を通り肝臓に達し肝炎を引き起こす[9]．潜伏期は約1ヶ月で，急性肝炎を呈する．発病率は低く，不顕性感染が多いと考えられており，妊婦で重症化する．我が国では当初HEVの感染は不明であったが，海外渡航歴が無く非A,B,C肝炎の患者血清を調べたところ，かなりの数で陽性例が見られた．さらに家畜のみならず，野生動物であるイノシシ，シカ肉を食してHEVに感染をし，肝炎を起こした例が報告されているので，我が国でもウイルスは存在すると思われる．また，述べたように発見当初はネズミ等のげっ歯類がキャリアとなりヒトに感染を示すと思われたが，哺乳類全てに広く感染をすることが判明し，世界中で家畜の陽性例が報告されるようになり，人獣共通伝染病の様相を呈してきた[10-12]．

3. ウイルス様中空粒子(VLP)

VLPとはウイルスの構造のみを有し，複製することの出来ない空の粒子である．最も多く報告のあるのはバキュロウイルスに構造タンパクを発現させて得られたもので，効率良くVLPの回収が出来る．VLPは構造が元のウイルスと同じであるために，本来の感染標的細胞への結合能やその他の特徴を保持している．VLPをワクチンとして利用すると自然感染と同様の免疫反応が期待できる．胃腸炎の原因ウイルスであるNorovirus（旧称，Norwalk-like viruses）のVLPでは経口投与によるワクチン試験が行われている[13]．VLPを用いたワクチンの利点としては他にはnoninfectious materialにもかかわらず細胞性免疫の誘導が認められること，免疫誘導にアジュバントが必要でないことも加えられよう．さらに概して安定であり，感染の危険性が無いので扱いも容易である．しかしながらウイルスの構造研究等では非常に有益なツールであるVLPもワクチンとして利用されるものは多くはない．その理由の一つに産生量の問題がある．実験に使用するには十分量を得ることが出来るが他のウイルスを用いたワクチンのような細胞培養系と比較すると極端に少量である．我々の経験上では1 mlの培養液での細胞培養で数μg得るのも困難である．ワクチンを接種するときのタンパク量を考えればワクチンとして使用するには心もとない．この点の克服がなされなければ実際の使用は困難であると思われる．

4. HEVのVLP

HEVのVLPは国立感染研の宮村博士らのグループによりOpen Reading Frame 2(ORF2)のバキュロウイルスによる発現系により樹立された[14]．このVLPは上述した産生量の問題点を克服しており，数百μgが細胞培養液1 mlより得られた．当初ORF2のC末の35個のアミノ酸を取り除いて作成しており，それではVLPの産生はTn5細胞からのみからであったが，その後52個のアミノ酸を削除することにより，他の昆虫細胞Sf9からもVLPの産生が認められた．我々はこの52個のアミノ酸を削除することにより，現在は500μg～1 mgを細胞培養液1 mlより得ることが可能であることを確認している．このHEV-VLPをマウスに経口投与すると血清中ならびに糞便中にHEV特異抗体が誘導され，HEV-VLPは本来の性質を維持していると考えられる[15]．さらにLi TCらはHEV-VLPを経口投与したサルではHEVに対する特異抗体の産生のみならず，HEVの感染に対して防御効果を示すことを報告した[16]．この様にHEV-VLPはウイルス本来の性質を維持しているのみならず，そのものがワクチンとして利用可能であることを示している．著者らはこのHEV-VLPの性質を利用し，粘膜免疫誘導可能な新規の経口ワクチンの開発を試み以下にその概要を述べる．

5. 他種ウイルスエピトープ表出キメラHEV-VLP

我々が最初に行ったのはこのHEV-VLPに他のウイルスエピトープを組み込んだキメラ

VLPの作成であり，経口投与においてエピトープ特異的粘膜ならびに全身的な免疫誘導の可能性を探った．作成を試みてから他に類似の報告を探してみるとキメラVLPの作成に成功している報告はなく[17]，エピトープ組み込みウイルスの作成は可能であるが，VLPの形成が見られなかった，もしくは産生量が極端に低下したという報告が多く，さらに挿入エピトープに関して免疫誘導が認められたという報告は皆無で，認められなかったと結論付けている．この様な報告から我々はVLP産生量に影響を及ぼさず，免疫系に認識されやすいようにVLP上に表出する形にエピトープを挿入することを試みた．

挿入するエピトープはherpes simplex virus (HSV)のglycoprotein DのB-cell tagエピトープ(QPELAPEDPED)とした．挿入位置は表出することを期待し疎水性領域とし，その中で酵素切断の容易な位置4ヶ所ならびにN末，C末の合計6ヶ所とした（Fig. 1）．これら6ヶ所全てにおいて細胞内でVLPの存在は認められたが，培養上清中のVLPの産生量は大きく異なった．このうち産生量が十分であるC末にtagを組み込んだVLPを精製し免疫沈降ならびにELISAでtagの発現を見たところ，どちらも反応を示したことから，tagエピトープが表出していることが示唆された(Fig. 2)．電子顕微鏡による観察ではエピトープ挿入キメラVLPと元々のVLPでは両者には見かけ上全く差が認められなかった（Fig. 3）．このキメラVLPをマウスに経口投与するとtag特異的IgG，IgAが血清中および腸管内容液より検出された（Fig. 4）．また，この産生された抗体のサブクラスを調べたところキメラVLP，オリジナルのVLPを投与されたマウスにおいて抗HEV抗体に対しては全く差が無くIgG1，IgA，IgMの順に高かった（Fig. 5）．

以上のようにHEV-VLPに他のエピトープを挿入したキメラVLPとし，それを経口投与することにより挿入エピトープに対する免疫反応が粘膜面および全身性に誘導できることが確認された．また，本稿では述べなかったが，挿入するエピトープを細胞傷害性Tリンパ球(CTL)エピトープにした場合，粘膜面および全身性にCTLが誘導されることも確認している．現在挿入可能箇所にどの位のサイズのアミノ酸が挿入できるかを検討しており，予備的実験ではアミノ酸50個程度ではVLPの産生量等には影響が無いことが確認されている．また，挿入可能箇所に同時に数種類のエピトープが挿入できるかについても検討している．

6. DNAワクチン封入HEV-VLP経口投与による粘膜免疫誘導

DNAワクチンは簡便であり，液性免疫および細胞性免疫の両者が誘導できること，更に安価であり，未だ重篤な副作用が報告されていないことから次世代のワクチンとして注目されている．しかしながらDNAワクチンの筋肉内や皮下接種等の全身投与では粘膜免疫の誘導は認めづらい．気管内投与では粘膜免疫の誘導が確認されているが，経口投与では困難である．著者らはこのDNAワクチンをHEV-VLPを用いることによりDNAワクチンを小腸粘膜上皮に運び，DNAワクチンでの粘膜免疫の誘導を試みた．

HEV-VLPは構成分子にCaイオンを結合しウイルス粒子を構成している．この事を利用しplasmid DNA溶液内でCaイオンをキレートし，一旦VLP構成分子間を広げ，その後Caイオンを再添加することによりDNAワクチンをHEV-VLP内に封入した（Fig. 6）．この操作を行ったVLPをCsClで比重遠心したところ2峰性のピークを示し，比重の重いピークにDNAが含まれていた．一方plasmid DNA溶液内でこの分子間を広げ再構築を行わなかったVLPではピークは一つでDNAも検出されなかった．封入されるDNA量を種々の大きさのDNAを用いて検討したところ50 μgのVLPに対しておおよそ18 μgのDNAが封入されていた(Fig. 7)．

このVLPを用いてDNAの細胞内への導入を *in vitro* で検討した．HEV-VLP内にGFP DNAを封入し種々の細胞株にトランスフェクトしGFPの発現を見たところ，使用した殆どの細胞株でGFPの発現が確認された(Fig. 8)．さらにヒトエイズウイルス（HIV）env発現DNAを同様に封入しマウスの経口投与したところ小腸粘膜上皮内でHIVenvの発現が確認された（Fig. 9）．この様に *in vitro*, *in vivo* のどちらでも細胞内へのDNAの導入，発現が認められたことから，HIVenv DNAワクチンを封入しマウスにおけるHIVenv特異的免疫反応を検討した．HIVenv DNAワクチンをHEVVLPに封入しマウスに一週間隔で4回，経口投与を行った．一回のDNAワクチン量は20 μgとした．血清中のHIVenv特異的IgGはDNAワクチン封入VLPの経口投与，皮下接種でどちらも同程度の誘導が認められたが，血清中のHIVenv特異的IgAは経口投与マウスにおいてのみ認められた．糞便中の特異的IgAも同様に経口投与マウスのみで認められ，糞便中のIgGは全てのマウスで認められなかった(Fig.10)．HIVenv特異的CTLも同様に検討した．マウスにHIVenv DNAワクチン封入VLPもしくはDNAワクチンそのものを経口投与し，脾細胞，腸間膜リンパ節細胞，パイエル板細胞のCTLの誘導を見たところ，HIVenv DNAワクチン封入VLP経口投与マウスではHIVenv特異的CTLが認められたが，DNAワクチンそのものを経口投与したマウスではCTLの誘導は一切認められなかった(Fig.11)．

以上のようにHEV-VLPは現在までに報告されているDNAワクチンのベクターとは全く異なる新規の粘膜免疫誘導可能な経口投与ワクチンベクターとしての可能性が示された．

7. おわりに

現在のように新興，再興感染症の危機を常に考えていかなければならない時代には，ワクチンベクターの研究に終りは無く，次々と新たなものを試みていく必要性がある．その条件としては安全性，コスト，手技の簡便さ等が要求される．その意味においては本稿で述べたVLPを用いることは魅力的であり，既存のVLPも産生量を増加させることが可能であればワクチンのみならず遺伝子治療のベクターとしても用いることが可能である．今後も研究の継続と実際の現場への利用に取り組みたいと考えている．

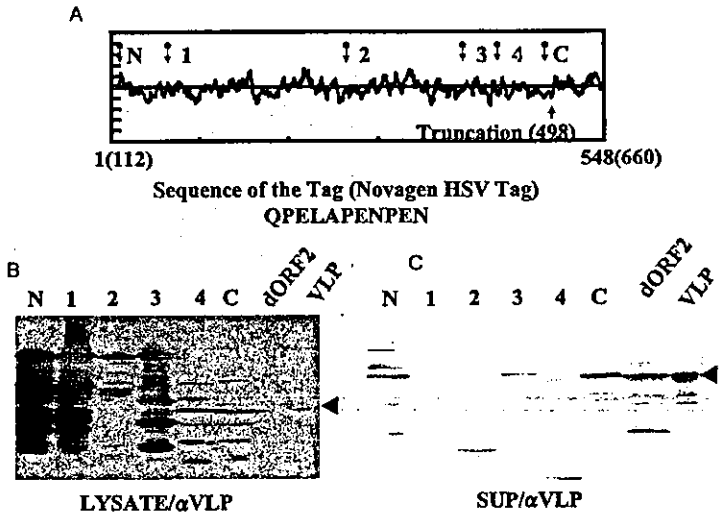

Fig. 1 キメラVLPの作成

A：TagエピトープはORF2の疎水性領域でN末，C末に加え1：Hind Ⅲ，2：Sac Ⅱ，3：BssH Ⅱ，4：Sac Ⅱの各酵素の切断siteを用いた．B：バキュロウイルス感染細胞のlysateを抗HEV抗体を用いたWestern blottingにてVLPの確認を行った．C：バキュロウイルス感染細胞培養上清を同様に抗HEV抗体を用いたWestern blottingを行い，VLPを確認した．

Fig. 2 培養上清の検討

培養上清から超遠心でペレットを得た．A：ペレットの電気泳動 B：ペレットの抗 HEV 抗体を用いた Western blotting. C：ペレットの抗 Tag 抗体を用いた Western blotting. D：ペレットの免疫沈降.

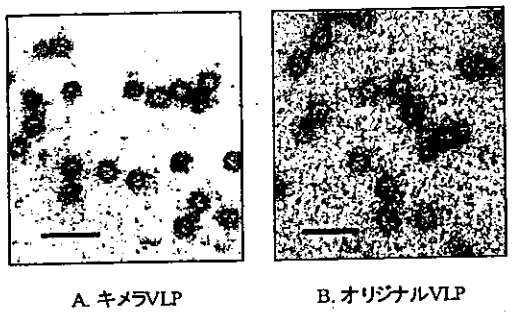

Fig. 3 キメラ VLP の電子顕微鏡による観察

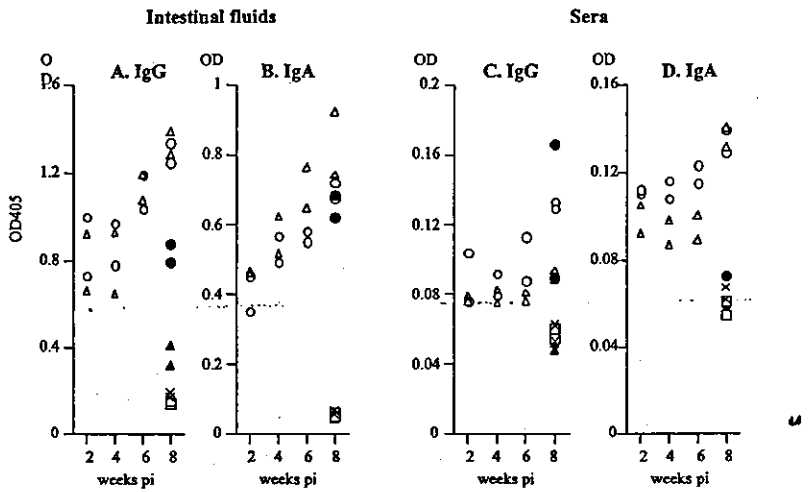

Fig. 4 キメラ VLP 経口投与マウスにおける抗体の誘導

キメラ VLP 経口投与マウスの抗 HEV 抗体（○），抗 Tag 抗体（△）．オリジナル VLP 経口投与マウスの抗 HEV 抗体（●），抗 Tag 抗体（▲）.

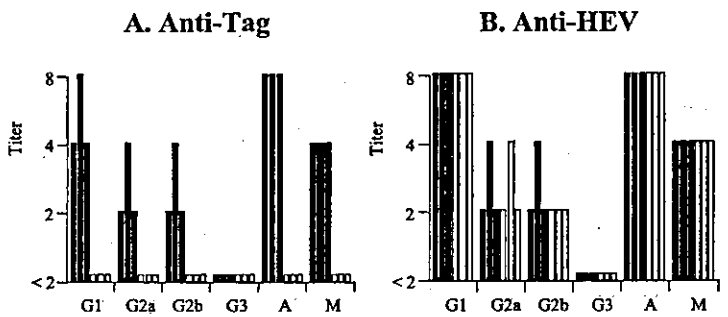

Fig. 5 キメラ VLP 経口投与マウスに産生された抗体のサブクラス

キメラ VLP 経口投与マウス（■），オリジナル VLP 経口投与マウス（□）.

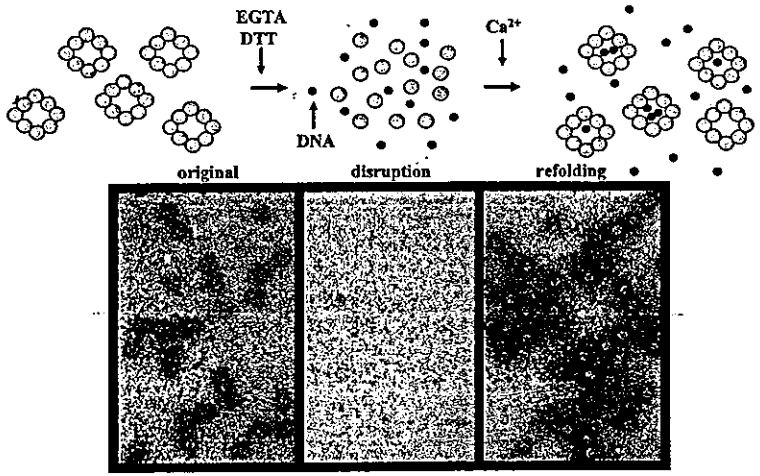

Fig. 6 DNA の HEV-VLP 内への封入
plasmid DNA 溶液内で Ca イオンをキレートし，分子間を広げその後 Ca を添加することにより plasmid DNA を HEV-VLP 内に封入した．

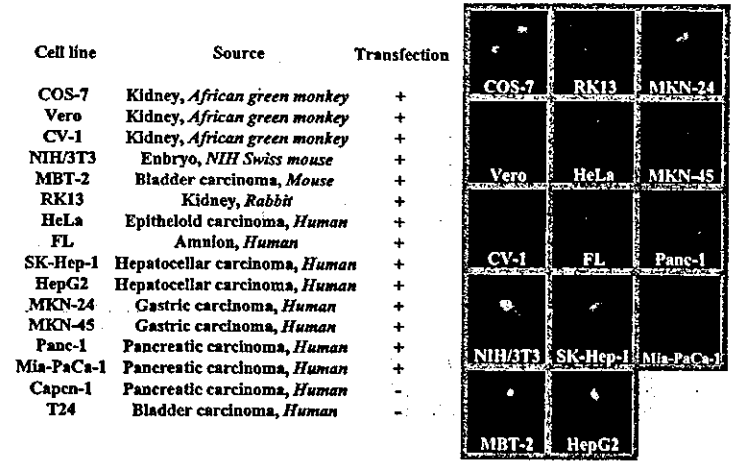

Cell line	Source	Transfection
COS-7	Kidney, *African green monkey*	+
Vero	Kidney, *African green monkey*	+
CV-1	Kidney, *African green monkey*	+
NIH/3T3	Enbryo, *NIH Swiss mouse*	+
MBT-2	Bladder carcinoma, *Mouse*	+
RK13	Kidney, *Rabbit*	+
HeLa	Epitheloid carcinoma, *Human*	+
FL	Amnion, *Human*	+
SK-Hep-1	Hepatocellar carcinoma, *Human*	+
HepG2	Hepatocellar carcinoma, *Human*	+
MKN-24	Gastric carcinoma, *Human*	+
MKN-45	Gastric carcinoma, *Human*	+
Panc-1	Pancreatic carcinoma, *Human*	+
Mia-PaCa-1	Pancreatic carcinoma, *Human*	+
Capcn-1	Pancreatic carcinoma, *Human*	-
T24	Bladder carcinoma, *Human*	-

Fig. 8 細胞株への HEV-VLP を用いた GFP DNA のトランスフェクション

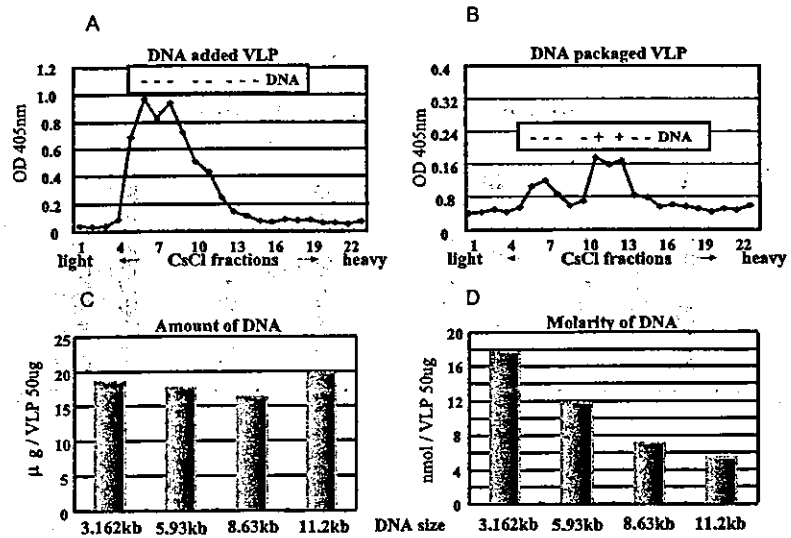

Fig. 7 plasmid DNA 封入 HEV-VLP
A. plasmid DNA 溶液内で Ca イオンをキレートしなかったときの CsCl 密度勾配遠心のフラクション．B. plasmid DNA 溶液内で Ca イオンをキレートしたときの CsCl 密度勾配遠心のフラクション．C. DNA サイズを変化させたときの封入された DNA 量（μg）．D. DNA サイズを変化させたときの封入された DNA の mol 濃度．

Fig. 9 HIVenv DNA 封入 HEV-VLP を経口投与されたマウスにおける HIVenv の発現．
a. HEV-VLP に封入せずに HIVenv DNA を経口投与されたマウス小腸上皮．b and c. HEV-VLP 封入 HIVenv DNA を経口投与されたマウス小腸上皮．矢印は HIVenv 発現細胞．

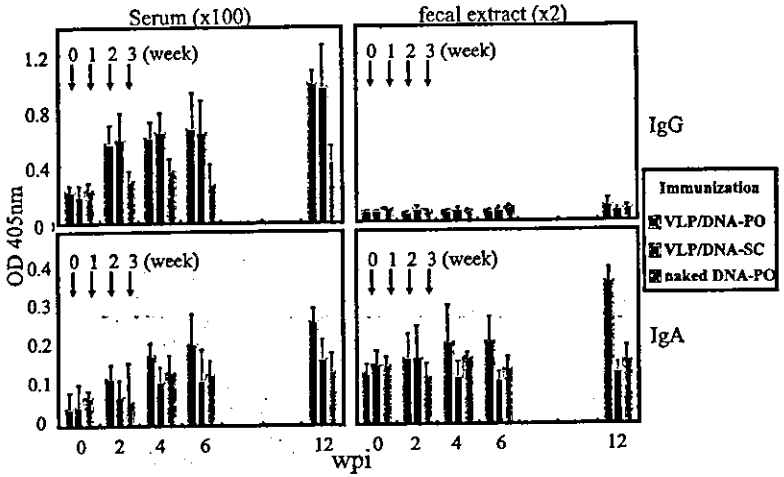

Fig.10 HEV-VLP 封入 HIVenv DNA 投与マウスにおける HIVenv 特異的抗体の産生.

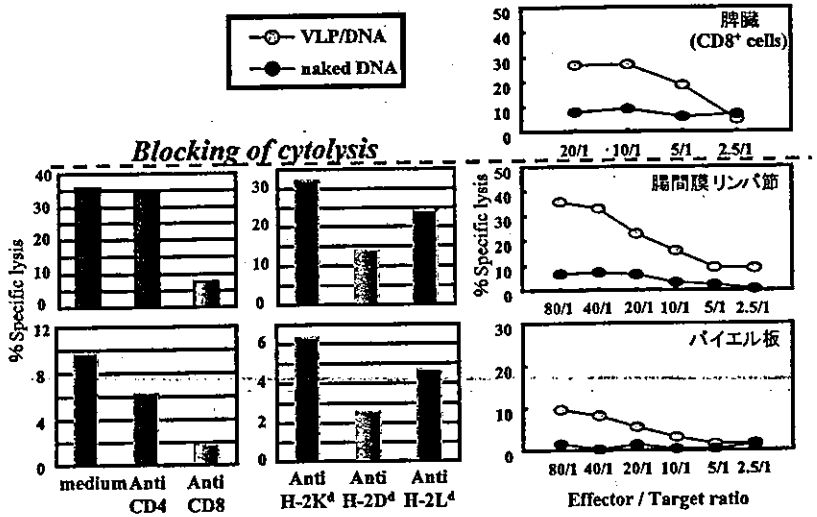

Fig.11 HIVenv DNA 経口投与マウスにおける HIVenv 特異的 CTL の誘導

文 献

1) Niikura, M., Takamura, S., Kim, G., Kawai, S., Saijo, M., Morikawa, S., Kurane, I., Tian-Cheng Li, Takeda, N. and Yasutomi, Y. Chimeric recombinant hepatitis E virus-like particles as an oral vaccine vehicle presenting foreign epitopes. Virology 293 : 273-280, 2002
2) Takamura, S., Niikura, M., Li, T. C., Takeda, N., Kusagawa, S., Takebe, Y., Miyamura, T., and Yasutomi, Y. DNA vaccine-encapsulated virus-like particles derived from an orally transmissible virus stimulates mucosal and systemic immune responses by oral administration. Gene Ther. 11 : 628-635, 2004
3) van Ginkel FL, Nguyen HH, McGhee JR. Vaccines for mucosal immunity to combat emerging infectious diseases. Emerging Infectious Disesses 6 : 123-132, 2000.
4) Yasutomi, Y., Koenig, S., Haun, S. S., Stover, C. K., Emini, E., Furest, T. R. and Letvin, N. L. Immunization with recombinant BCG-SIV elicits SIV-specific cytotoxic T lymphocytes in rhesus monkey. J. Immunol. 150 : 3101-3107, 1993.
5) Uno-Furuta, S., Matsuo, K., Kim, G., Tamaki, S., Takamura, S., Kamei, A., Kuromatsu, I., Kaito, M., Matsuura, Y., Miyamura, T., Adachi, Y., and Yasutomi, Y. Vaccine 21 : 3149-3156, 2003.
6) Stohr k., MelsinF-X. Progress and setbacks in the oral immunization of foxes against rabies in Europe. Vet. Rec. 139 : 32-35, 1996.
7) Muller T., Schulter H. Oral immunization of red foxes (Vulpes vulpes L) in Europe : A review. J. Etlik. Vet. Microbiol. 9 : 35-59, 1998.
8) MacInnes CD, Smith SM, Tinline RR, Ayers NR, Bachmann P, Ball DGA, Calder LA, Crosgrey SJ, Fielding C, Hauschildt P, Honig JM, Johnston DH, Lawson KF, Nunan CP, Pedde MA, Pond B, Stewart RB, Voigt DR. Elimination of rabies from foxes in eastern Ontario. J. Wild. Dis. 37 : 119-132, 2001.
9) Berke T., Matson DO. Reclassification of the Caliciviridae into distinct genera and exclusion of hepatitis E virus from the family on the basis of comparative phylogenetic analysis. Arch. Virol. 145 : 1421-1436, 2000.
10) Meng XJ., Purcell RH., Halbur PG., Lehman JR, Webb DM, Tsareva TS, Haynes JS, Thacker BJ, Emerson SU. A novel virus in swine is closely related to the human hepatitis E virus. Proc. Natl. Acad. Sci. USA. 94 : 9860-9865, 1997.
11) Okamoto H., Takahashi M., Nishizawa T., Fukai K., Muramatsu U., Yoshikawa A. Analysis of the complete genome of indigenous swine hepatitis E virus isolated in Japan. Biochem. Biophys. Res. Commun. 289 : 929-936, 2001.
12) Nishizawa T., Takahashi M., Mizuo H., Miyajima H., Gotanda Y., Okamoto H. Characterization of Japanese swine and human hepatitis E virus isolated genotype IV with 99% identity over the entire genome. J. Gen. Virol. 84 : 1245-1251, 2003.
13) Ball JM., Graham DY., Opekun AR., Gilger MA., Guerrero RA., Estes MK. Recombinant Norwalk virus-like particles given orally to volunteers : phase I study. Gastroenterology 117 : 40-48, 1999.
14) Li TC., Yamakawa Y., Suzuki K., Tatsumi M., Razak MA., Uchida T., Takeda N., Miyamura T. Expression and self-assembly of empty virus-like particles of hepatitis E virus. J. Virol. 71 : 7207-7213, 1997.
15) Li TC., Takeda N. Miyamura T. Oral administration of hepatitis E virus-like particles induces a systemic and mucosal immune response in mice. Vaccine 19 : 3476-3484, 2001.
16) Li TC., Suzaki Y., Ami Y., Dhole TN., Miyamura T., Takeda N. Protection of cynomologous monkeys against HEV infection by oral administration of recombinant hepatitis E virus-like particles. Vaccine 22 : 370-377, 2004.
17) Modelska A., Dietzschold B., Sleysh N., Fu Z. F., Steplewski K., Hooper D. C., Koprowski H., Yusibov V. Immunization against rabies with plant-derived antigen. Proc. Natl. Acad. Sci. USA 95 : 2481-2485, 1998.

Available online at www.sciencedirect.com
SCIENCE DIRECT
Virology 319 (2004) 163–175
VIROLOGY
www.elsevier.com/locate/yviro

Codon optimization of the HIV-1 *vpu* and *vif* genes stabilizes their mRNA and allows for highly efficient Rev-independent expression

Kim-Lien Nguyen,[a] Manuel Llano,[b] Hirofumi Akari,[a] Eri Miyagi,[a] Eric M. Poeschla,[b] Klaus Strebel,[a] and Stephan Bour[a,c,*]

[a] *Viral Biochemistry Section, Laboratory of Molecular Microbiology, National Institutes of Allergy and Infectious Diseases, Bethesda, MD 20892, USA*
[b] *Molecular Medicine Program, Mayo Clinic, Rochester, MN 55905, USA*
[c] *Bioinformatics Core, Laboratory of Molecular Microbiology, National Institutes of Allergy and Infectious Diseases, Bethesda, MD 20892, USA*

Received 25 September 2003; returned to author for revision 14 November 2003; accepted 17 November 2003

Abstract

Two HIV-1 accessory proteins, Vpu and Vif, are notoriously difficult to express autonomously in the absence of the viral Tat and Rev proteins. We examined whether the codon bias observed in the *vpu* and *vif* genes relative to highly expressed human genes contributes to the Rev dependence and low expression level outside the context of the viral genome. The entire *vpu* gene as well as the 5′ half of the *vif* gene were codon optimized and the resulting open reading frames (ORFs) (*vphu* and *hvif*, respectively) were cloned in autonomous expression vectors under the transcriptional control of the CMV promoter. Codon optimization efficiently removed the expression block observed in the native genes and allowed high levels of Rev- and Tat-independent expression of Vpu and Vif. Most of the higher protein levels detected are accounted for by enhanced steady-state levels of the mRNA encoding the optimized species. Nuclear run-on experiments show for the first time that codon optimization has no effect on the rate of transcriptional initiation or elongation of the *vphu* mRNA. Instead, optimization of the *vpu* gene was found to stabilize the *vphu* mRNA in the nucleus and enhance its export to the cytoplasm. This was achieved by allowing the optimized mRNA to use a new CRM1-independent nuclear export pathway. This work provides a better understanding of the molecular mechanisms underlying the process of codon optimization and introduces novel tools to study the biological functions of the Vpu and Vif proteins independently of other viral proteins.
Published by Elsevier Inc.

Keywords: HIV-1; Vpu; Codon optimization; mRNA

Introduction

Expression of the HIV-1 genes is tightly controlled, allowing exquisite temporal modulation of regulatory and structural gene expression. Two regulatory proteins of HIV, Tat and Rev, have a critical role in the transcriptional and posttranscriptional regulation of viral gene expression. Tat acts as a transcriptional activator of the HIV long terminal repeat (LTR) by binding to the TAR element found at the 5′ end of all HIV-1 transcripts (Jeang et al., 1999). Transcription of HIV genes is initiated from a single promoter located in the 5′ LTR. The primary transcript corresponds to the full-length genomic RNA and individual HIV-1 mRNAs coding for the nine viral proteins or protein precursors are generated by differential splicing of the primary transcript. Early gene products such as Tat, Rev, and Nef are translated from doubly spliced messages that are efficiently exported from the nucleus. Unspliced and singly spliced messages encoding Vif, Vpr, Vpu, and the viral Gag, Pol and Env contain an RNA stem–loop structure termed the Rev-responsive element (RRE) located in the *env* gene. Mechanistically, Rev has been shown to facilitate HIV RNA export by binding to the RRE and by simultaneously interacting with the CRM1/Ran complex, which in turn interacts with components of the nuclear pore complex to mediate the energy-dependent translocation of the RNA molecule into the cytoplasm (Kjems and Askjaer, 2000).

While recent data have clarified the role of Rev in facilitating RRE-containing RNA nuclear export, much remains to be learned to fully understand the reason for the

* Corresponding author. Viral Biochemistry Section, Laboratory of Molecular Microbiology, NIH/National Institutes of Allergy and Infectious Diseases, 4 Center Drive, Room 337, Bethesda, MD 20892-0460. Fax: +1-301-402-0226.
E-mail address: sbour@niaid.nih.gov (S. Bour).

0042-6822/$ - see front matter. Published by Elsevier Inc.
doi:10.1016/j.virol.2003.11.021

Rev dependence of HIV messages. Indeed, numerous studies have indicated that the RRE is not the main element responsible for nuclear retention of viral mRNA in the absence of Rev (Chang and Sharp, 1989). Instead, regions of high AU content (Maldarelli et al., 1991; Schwartz et al., 1992a) as well as AUUUA motifs (Schneider et al., 1997), collectively referred to as *cis*-acting inhibitory elements (INS), have been identified and largely account for the nuclear retention of unspliced and singly spliced HIV-1 mRNAs. Selective inactivation of the INS in HIV-1 *gag* and *pol* genes has resulted in enhanced levels of Rev-independent expression and correlated with increased levels of cytoplasmic mRNA (Schneider et al., 1997). Reduction of the AU content and removal of AUUUA sequences can also be achieved globally on mRNA sequences by a process referred to as codon optimization. This strategy does not require the prior identification and mapping of INS sequences and involves the optimization of the viral coding sequence to approximate the codon usage observed in highly expressed human genes (Kypr and Mrazek, 1987). When applied to HIV-1 genes, this strategy has allowed increased Rev-independent expression of the Env, Gag, and Pol gene products (Haas et al., 1996; Kotsopoulou et al., 2000). The mechanism responsible for enhanced expression of codon-optimized genes remains poorly defined. Indeed, while codon replacement in the HIV-1 *env* gene led to increased protein levels with no detectable effect on RNA stability (Haas et al., 1996), increased mRNA levels in the cytoplasm accounted for most of the enhanced expression of the codon-optimized *gag* and *pol* genes (Kotsopoulou et al., 2000; Schneider et al., 1997). Two main mechanisms have been proposed to account for this enhanced cytoplasmic export of codon-optimized RNA. A first factor is the stabilization of the nuclear RNA due to a reduction in the global AU content as well as the inactivation of AUUUA AU-rich elements (AREs). The negative effect of AU-rich regions and various ARE motifs on RNA stability is well documented (Hollams et al., 2002). They often account for the inherent instability of a given RNA and can confer instability to otherwise stable RNA. Second, codon-optimized HIV-1 Gag mRNAs gain access to Rev- and CRM1-independent nuclear export pathways, leading to more efficient transport of unspliced RNA to the cytoplasm (Graf et al., 2000). With the notable exception of HIV genes, most of the AU-rich and ARE sequences have been located in the 3′ untranslated region (UTR) of cellular messages.

We sought to clarify the molecular mechanisms responsible for enhanced expression following codon optimization and its relationship with the presence of INS or AUUUA repeats. The Vpu protein is translated from a bicistronic mRNA that also contains the *env* open reading frame (ORF) (Schwartz et al., 1992b). Therefore, despite the fact that the RRE is at a considerable distance from the *vpu* ORF, expression of Vpu in its native context is rendered Rev-responsive. The Vpu and Vif proteins express poorly from autonomous expression vectors, suggesting that the Rev/RRE serve to relieve an inherent expression inhibitor present in the ORF of these two accessory proteins.

The ability of HIV-1 Vif to promote viral infectivity as well as the property of Vpu to enhance viral particle release (Bour and Strebel, 2000) make these two factors important for many applications such as gene therapy. Yet, low expression levels of Vpu and Vif have hampered not only the molecular characterization of their biological functions, but have also prevented their use in the production of recombinant retroviral particles. To overcome these limitations, we have generated codon-optimized *vpu* and *vif* genes that bear no significant nucleotide sequence homology with their natural counterparts. We show that the proteins produced by these synthetic genes are highly expressed in autonomous expression systems and fully functional. We further demonstrate that the inefficient expression of Vpu and Vif proteins from their native mRNA is mainly due to RNA instability caused by poor cytoplasmic export in the absence of the Rev protein. Nuclear run-on experiments further demonstrate for the first time that codon optimization does not alter the initiation or elongation of mRNA. In fact, the mRNA export inhibition observed for native *vpu* and *vif* sequences is relieved by codon optimization by allowing the synthetic RNA messages to use a CRM1-independent nuclear export pathway. These data not only provide valuable information regarding the mechanism of codon optimization but also provide the first example of codon optimization of HIV-1 accessory proteins for which no INS or ARE have been documented. Finally, this study provides two novel vectors for the autonomous expression of the viral Vpu and Vif proteins.

Results

Codon optimization enhances the levels of Vpu and Vif proteins

To determine the effect of codon optimization on protein synthesis, we examined the rate of synthesis as well as the steady-state levels of the synthetic genes under the transcriptional control of the CMV IE promoter. For that purpose, the *vpu* and *vif* genes and their optimized *vphu* and *hvif* counterparts were cloned in the pcDNA3.1 vector. Reference vectors for Vpu expression included the full-length HIV-1 molecular clone pNL4-3 as well as a pNL4-3 derivative, pNL-A1, lacking the *gag* and *pol* genes (Strebel et al., 1988). Vpu-defective variants of pNL4-3 and pNL-A1 (pNL4-3/Udel and pNL-A1/Udel, respectively) were included as negative controls. The vectors were transfected into HeLa cells and analyzed by Western blotting with a Vpu-specific polyclonal antibody. As shown in Fig. 1A, the pcDNA-Vphu vector, bearing the codon-optimized *vpu* ORF expressed Vpu at levels comparable to that observed for wild-type Vpu in its natural context (pNL4-3 and pNL-A1). No Vpu expression was detectable from the pcDNA-Vpu construct bearing the wild-type *vpu* ORF in the same vector context as pcDNA-

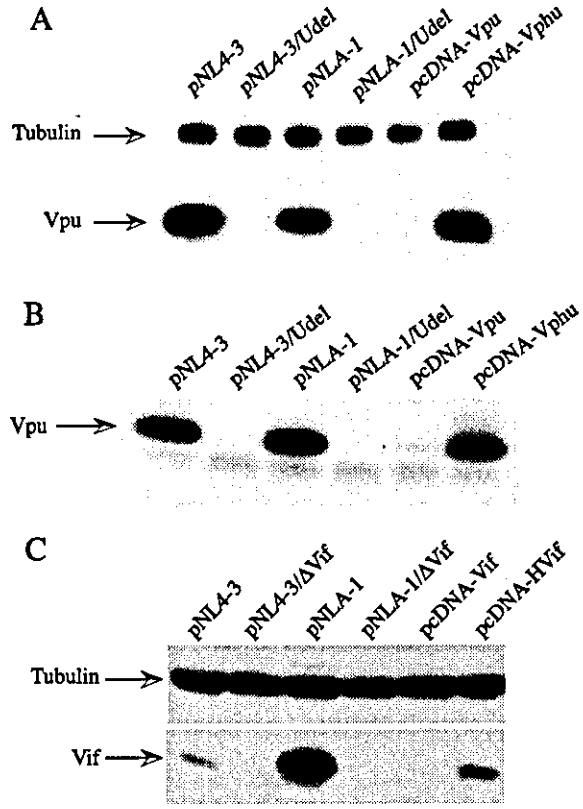

Fig. 1. Effect of codon optimization on Vpu and Vif expression. (A) Steady-state Vpu expression levels. HeLa cells were transfected with 4 μg of pNL4-3, pNL4-3/Udel, pNL-A1, or pNL-A1/Udel, and 1.33 μg of pcDNA-Vpu, or pcDNA-Vphu. Cell lysates were analyzed 24 h posttransfection by Western blotting using a rabbit anti-Vpu antiserum (U2-3). The blots were also probed with an anti-α-tubulin antibody as a loading control. (B) Rate of translation of Vpu. HeLa cells transfected as above were labeled with 200 μCi of Trans-^{35}S-methionine for 1 h at 37°C. Cell lysates were immunoprecipitated with the U2-3 Vpu antibody, separated on 12.5% SDS-polyacrylamide gels, and the bands visualized by fluorography. (C) Steady-state Vif expression levels. HeLa cells were transfected with 4 μg pNL4-3, pNL4-3/Vif(−), pNLA-1, and pNLA-1/ΔVif, or 2 μg of pcDNA-Vif and pcDNA-HVif. Cell lysates were analyzed 24 h posttransfection by Western blot with 1:10,000 dilution of rabbit anti-Vif polyclonal serum.

Vphu. These data indicate that codon optimization of the *vpu* gene relieved an expression block that prevented Vpu from being expressed in the absence of Rev.

We next examined whether this higher steady-state level of Vpu was due to enhanced protein synthesis or improved stability of the optimized protein. To this end, transfected HeLa cells were metabolically labeled with [^{35}S]-methionine for 1 h and subjected to anti-Vpu immunoprecipitation. As shown in Fig. 1B, the results of the metabolic labeling are remarkably similar to that of the Western blot experiment presented in Fig. 1A. These data strongly suggest that the codon optimization affected the rate of synthesis but not the stability of the synthetic species. Similar experiments were performed for the *vif* gene (Fig. 1C). Partial optimization of *vif* led to a significant enhancement of protein synthesis from the CMV promoter (pcDNA-HVif), as compared to the wild-type gene in the same promoter context (pcDNA-Vif). Levels of Vif protein expression from the pcDNA-HVif construct were similar to that observed in the native context of the full-length pNL4-3 (Fig. 1C).

The codon-optimized Vpu and Vif products are biologically active

We next examined whether the codon-optimized Vpu and Vif proteins were biologically active when expressed autonomously from the CMV promoter-driven pcDNA vector. The ability of the Vphu protein to enhance viral particle release was first examined in HeLa cells cotransfected with the Vpu-defective pNL4-3/Udel construct and increasing amounts of pcDNA-Vphu. Reverse transcriptase activity measured in the culture supernatants 24 h postinfection showed that wild-type NL4-3 expressing Vpu released close to 4-fold more viral particles than the NL4-3/Udel (Fig. 2A). The addition of increasing amounts of the non-optimized pcDNA-Vpu construct had little effect on the efficiency of viral particle release (Fig. 2A, pNL4-3/Udel + pcDNA-Vpu). In contrast, as little as 0.3 μg of co-transfected pcDNA-Vphu enhanced NL4-3/Udel particle release to the levels observed with wild-type NL4-3 expressing authentic Vpu in its native context (Fig. 2A, pNL4-3/Udel + pcDNA-Vphu). The dosage of the pcDNA-Vphu construct showed that maximum effect was observed with 0.3–0.6 μg of transfected plasmid. At the higher concentration of 1.2 μg, Vphu was reproducibly observed to be less effective [Fig. 2A, pNL4-3/Udel + pcDNA-Vphu (1.2 μg)]. Because Vpu can induce apoptosis of cells (Akari et al., 2001; Bour et al., 2001), the low particle release efficiency observed in the presence of 1.2 μg of pcDNA-Vphu is likely due to cytotoxic effects generated by the high levels of Vpu (Fig. 2B).

To confirm that the increase in cell-free reverse transcriptase activity observed in Fig. 2A was indeed due to the positive effect of Vphu on particle release, pulse-chase experiments were performed. HeLa cells were transfected with the wild-type HIV-1 molecular clone NL4-3 or its Vpu-defective counterpart NL4-3/Udel in the presence of either pcDNA-Vpu or pcDNA-Vphu. Cells were pulse-labeled for 30 min with [^{35}S]-methionine and chased for 4 h. At each time point indicated in Fig. 2C, samples of the cell and supernatant fractions were collected, lysed, and subjected to immunoprecipitation with HIV-positive human sera. The immunoprecipitates were separated on SDS-PAGE and visualized by fluorography (Fig. 2C). As shown in panel 1, progeny virus production, as evidenced by the pelletable p24 secreted in the VIRUS fraction, is enhanced by the presence of Vpu in NL4-3, as compared to the Vpu-defective NL4-3/Udel. When pcDNA-Vpu was provided in trans to pNL4-3/Udel, no significant enhancement of particle release was observed (Fig. 2C, pNL4-3/Udel + Vpu). In contrast, cotransfection of pcDNA-Vphu led to a significant increase in particle release, concomitant with the detection of Vphu protein in the cell fraction (Fig. 2C, pNL4-3/Udel + Vphu).

Viral Gag proteins detected in Fig. 2C were quantified and the particle release efficiency was calculated as the ratio between Gag proteins in the VIRUS fraction and the total Gag proteins in the CELL + VIRUS fractions. When plotted as a function of chase time, the particle release ratio of pNL4-3/Udel showed a 6-fold increase in the presence of pcDNA-Vphu, versus a modest 2-fold increase in the presence of pcDNA-Vpu (Fig. 2D). The latter phenomenon was at least in part due to the known enhancing effect of Tat on transcriptional activity of the CMV promoter leading to low levels of Vpu expression from the pcDNA-Vpu plasmid (Kim and Risser, 1993). We and others have previously reported that Vpu has the ability to enhance particle release of diverse retroviruses, including HIV-2 (Bour and Strebel, 1996; Gottlinger et al., 1993; Ritter et al., 1996). As expected, pulse-chase experiments performed with HIV-2 molecular clones showed a close to 8-fold particle release enhancement in the presence of pcDNA-Vphu but not of pcDNAVpu (data not shown). Taken together, the HIV-1 and HIV-2 particle release data indicate that codon-optimized *vpu* gene expressed under the transcriptional control of the CMV promoter behaves similarly to its wild-type counterpart in the context of the full-length HIV-1 genome. The engineered *vpu* gene therefore represents a functional homologue to the native *vpu* gene without a requirement for coexpression of the viral Tat and Rev proteins.

We next examined whether the partially optimized *vif* gene was biologically functional. The Vif protein functions in the virus producer cell and its presence is essential for viral infectivity. Virus produced in restrictive cell types such as H9 cells requires the presence of a functional Vif protein for the production of infectious progeny. The biological functionality of the codon-optimized HVif was tested by transfecting the restrictive H9 cells with plasmids encoding either the full-length NL4-3 or its Vif-defective counterpart (pNL4-3/Δvif). All molecular clones employed in this experiment were defective for *env* (NL4-3K1 variants) and pseudotyped with the vesicular stomatitis virus glycoprotein G (VSV-G) for subsequent infection of MAGI cells. Plasmids encoding either the wild-type or codon-optimized Vif were provided in trans. Transfected H9 cells were lysed 24 h posttransfection and Vif expression was

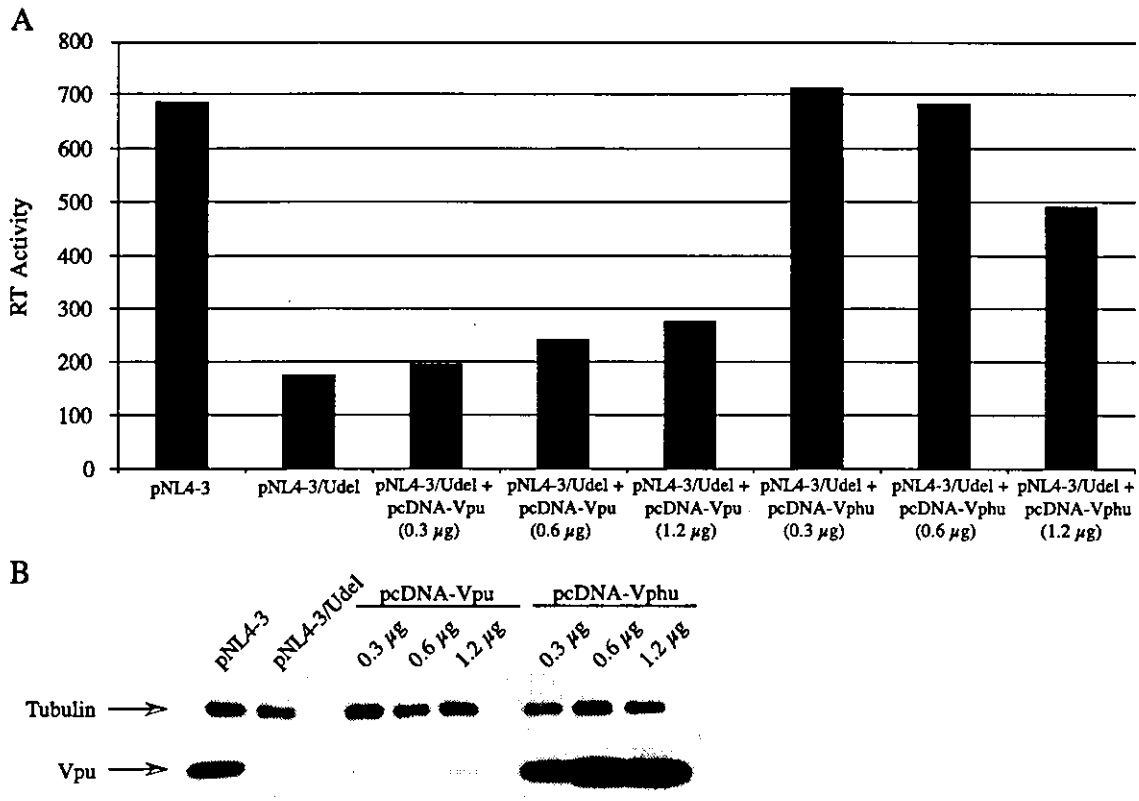

Fig. 2. Effect of Vphu on HIV-1 particle release. (A) HeLa cells were transfected with 3 μg of pNL4-3 or pNL4-3/Udel and either 1.2 μg of pcDNA3.1 (pNL4-3 and pNL4-3/Udel) or the indicated amounts of pcDNA-Vpu (pNL4-3/Udel + Vpu) or pcDNA-Vphu (pNL4-3/Udel + Vphu). Reverse transcriptase assay was performed on 10 μl of culture medium. (B) Five micrograms of cells lysates from transfection in A was separated on 12.5% SDS-PAGE, transferred to nitrocellulose membranes, and probed in Western blot with polyclonal antibodies against Vpu or tubulin. (C) HeLa cells were transfected as in A, labeled with 200 μCi of Trans-^{35}S-methionine for 30 min, and chased for a total of 4 h. At each indicated time point, cells and virus were lysed in 1% NP-40 lysis buffer and immunoprecipitated with HIV-positive human serum (TP), separated on 12.5% polyacrylamide-SDS gels, and visualized by fluorography. The positions of the Env and major Gag products are indicated on the left. (D) Particle release efficiency was calculated as the ratio of Gag proteins in the VIRUS fraction versus total Gag proteins in the CELL and VIRUS fractions and plotted as a function of chase time.

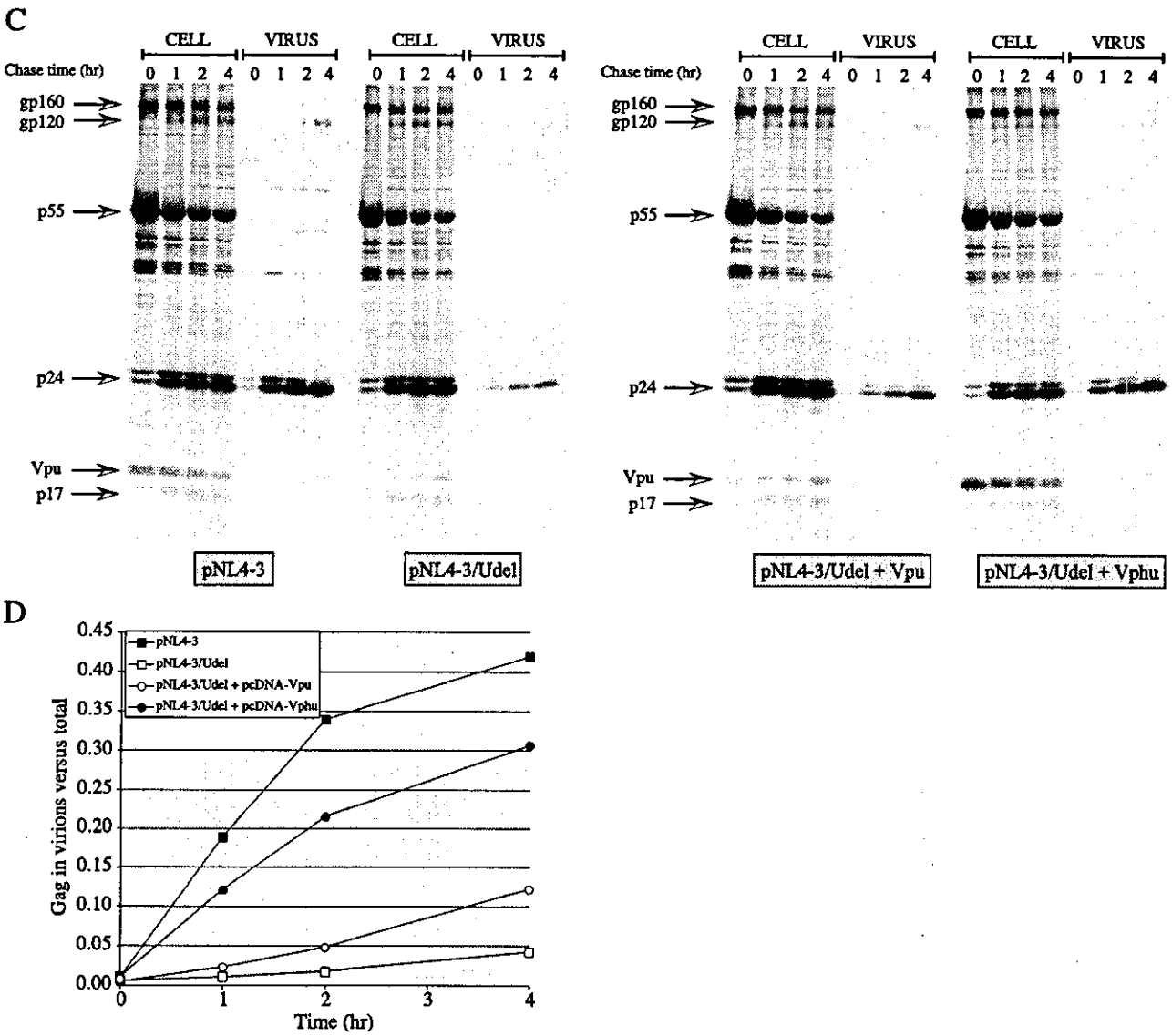

Fig. 2 (*continued*).

examined by Western blotting. As shown in Fig. 3A, the major p55, p41, and p24 Gag products were detected in similar quantities for all samples. Vif expression was efficient in the case of the NL4-3K1 molecular clone (Fig. 3A, lane 1) but absent for the NL4-3/Δvif variant, even in the presence of the non-optimized pcDNA-Vif construct (Fig. 3A, lanes 2 and 3). When provided in trans, the pcDNA-HVif plasmid encoding codon-optimized *vif* produced detectable levels of Vif, albeit at lower levels than the wild-type virus (Fig. 3A, lane 4). Progeny virus collected 24 h posttransfection was quantified and viral infectivity was assessed by MAGI assay. As shown in Fig. 3B, the absence of Vif in NL4-3K1/Δvif led to a 77% reduction in infectivity. Providing Vif in trans expressed from the pcDNA-Vif plasmid had no significant effect on the infectivity of the NL4-3/ΔVif-produced virus (Fig. 3B, lane 3). In contrast, the presence of pcDNA-HVif restored viral infectivity to over 80% of the level observed for wild-type virus (Fig. 3B, lane 4). The pcDNA-HVif-optimized construct therefore demonstrated viral infectivity enhancing effects at levels close to the wild-type virus.

Effect of optimization on transcription

Codon optimization of the *vpu* and *vif* ORFs led to a remarkable enhancement in the rate of synthesis of the respective proteins. However, it remains unclear whether this was due to enhanced translation of the synthetic mRNA or higher steady-state levels of the mRNA itself. While the term codon optimization suggests a main effect on translation (Haas et al., 1996), it has been suggested that codon optimization could also lead to higher levels of cytoplasmic mRNA (Kotsopoulou et al., 2000). To address the mechanism by which codon optimization of *vpu* and *vif* enhanced

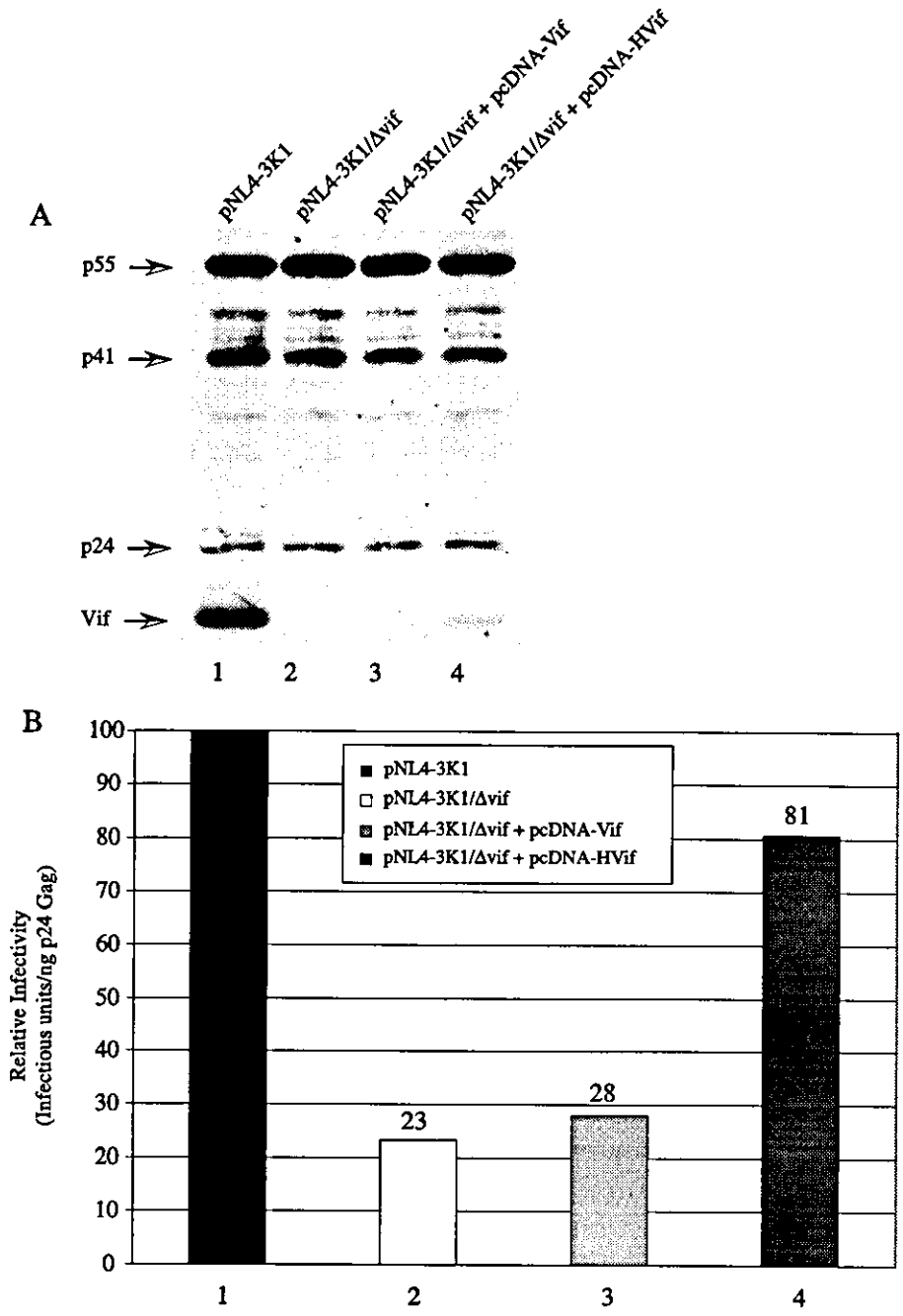

Fig. 3. Biological activity of pcDNA-HVif. (A) Pseudotyped viruses were obtained by transfecting 4×10^6 H9 cells with (lane 1) pNL43-K1, pCMV-G, and pcDNA; (lane 2) pNL43-K1/Δvif, pCMV-G, and pcDNA; (lane 3) pNL43-K1/Δvif, pCMV-G, and pcDNA-vif; (lane 4) pNL43-K1/Δvif, pCMV-G, and pcDNA-HVif (5 mg each, 15 mg in total) by electroporation. Transfected H9 cells were lysed 24 h posttransfection, separated on a 12.5% polyacrylamide-SDS gel, probed with anti-Vif antibody and anti-p24Gag, and visualized by ECL chemiluminescence. The position of the p55, p41, and p24 major Gag products as well as Vif are indicated on the left. (B) Twenty-four hours posttransfection, culture supernatants were harvested, filtered, and quantified by p24 ELISA. Viral infectivity was determined by MAGI assay. Averages of three independent experiments are shown.

protein expression, we first examined the steady-state levels of the respective mRNA. HeLa cells were transfected with plasmids encoding either the native (pcDNA-Vpu) or optimized (pcDNA-Vphu) *vpu* gene. Total and cytoplasmic RNA was extracted, separated by gel electrophoresis and probed in Northern blotting with a 212-nt probe mapping to the 5′ UTR (Fig. 4A). As expected, no *vpu*-specific band was detected in the pcDNA 3.1(−) empty vector control. Interestingly, little or no *vpu*-specific RNA was detected from cells transfected with pcDNA-Vpu, suggesting that the lack of protein expression from this vector is mainly due to its inability to accumulate *vpu*-specific mRNA in the nucleus or cytoplasm. In marked contrast, RNA produced by the codon-optimized pcDNA-Vphu was abundant both in the

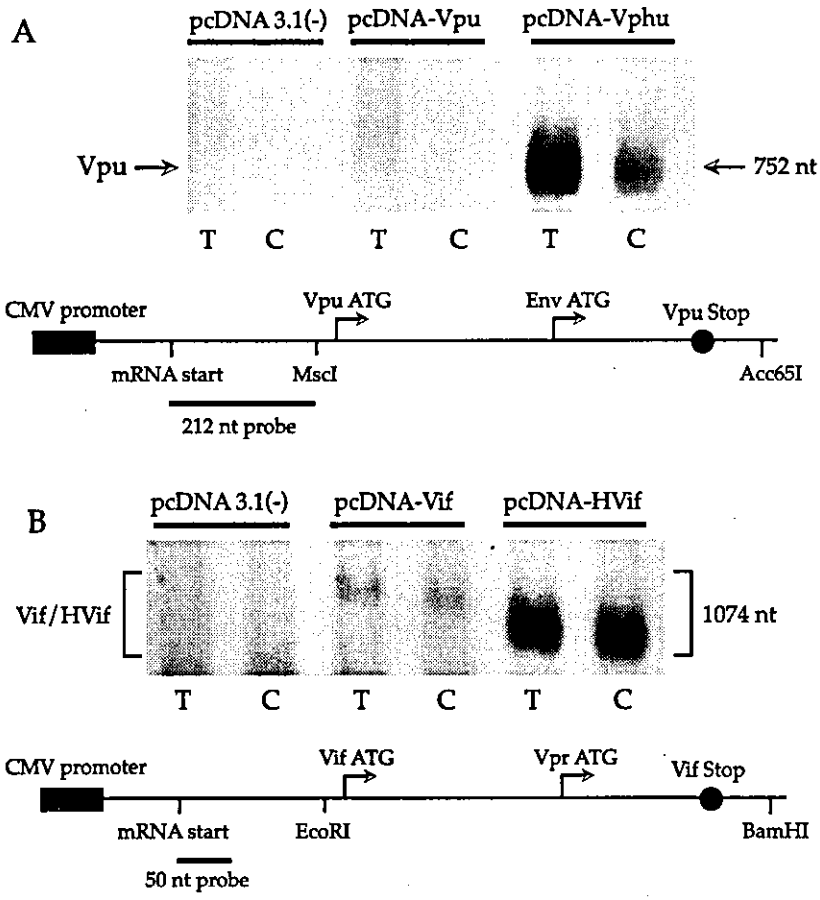

Fig. 4. Effect of codon optimization on RNA steady-state levels. (A) Vpu and Vphu RNA levels. HeLa cells were transfected with 2 μg pcDNA3.1, pcDNA-Vpu, or pcDNA-Vphu. Five micrograms of total and cytoplasmic RNA isolated 24 h posttransfection was separated on a 1% denaturing agarose gel and transferred onto nitrocellulose membrane. A 212-bp biotinylated DNA probe containing sequences complementary to the 5′ UTR of Vpu and Vphu was hybridized to the RNA at 42 °C overnight and detected by chemiluminescence. (B) Comparison of total versus cytoplasmic Vif/HVif RNA levels. HeLa cells were transfected with 2 μg pcDNA3.1, pcDNA-Vif, or pcDNA-HVif. Five micrograms of total and cytoplasmic RNA isolated 24 h posttransfection was separated on a 1% denaturing agarose gel and transferred onto nitrocellulose membrane. A 60-bp biotinylated DNA probe containing sequences complementary to the 5′ UTR of Vif and HVif was hybridized to the RNA at 37 °C overnight and detected by chemiluminescence.

total and cytoplasmic fractions. Similar experiments were performed for the optimized *vif* gene (Fig. 4B). In the case of *vif*, low RNA expression could be detected from the non-optimized pcDNA-Vif construct. However, as was the case for *vpu*, a significant enhancement of both total and cytoplasmic RNA levels was observed following codon optimization (Fig. 4B, pcDNA-HVif). These data strongly suggest that the main effect of codon optimization of both the *vpu* and *vif* genes is at the RNA level whereby higher cytoplasmic mRNA steady-state levels could account for most of the observed increase in protein levels.

To rule out the possibility that the lack of RNA expression from the non-optimized species was due to low transfection efficiency or instability of the plasmid DNA, Southern blots were performed with low molecular weight DNA from cells transfected with both the authentic and codon-optimized Vpu-expressing constructs. No difference was observed in the nuclear accumulation of the pcDNA-Vpu and pcDNA-Vphu plasmids, indicating that both constructs were properly transfected and had similar stability in cells (data not shown).

Effect of codon optimization on transcriptional initiation and elongation

To better define the mechanism by which codon optimization enhances the steady-state levels of *vpu* mRNA, we performed nuclear run-on (NRO) experiments to assess the rate of initiation and elongation of the *vpu* message. To provide a global view of the transcriptional process, multiple DNA probes were used that spanned the entire *vpu* RNA. As shown in Fig. 5A, three separate probes were designed for the *vpu* and *vphu* messages. The 5′ UTR probe spans the transcriptional initiation site and provides a measure of the early transcription events. The 5′ and 3′ coding probes allowed us to monitor the elongation efficiency of the transcribed RNA and assess whether premature termination was occurring. A probe mapping to the

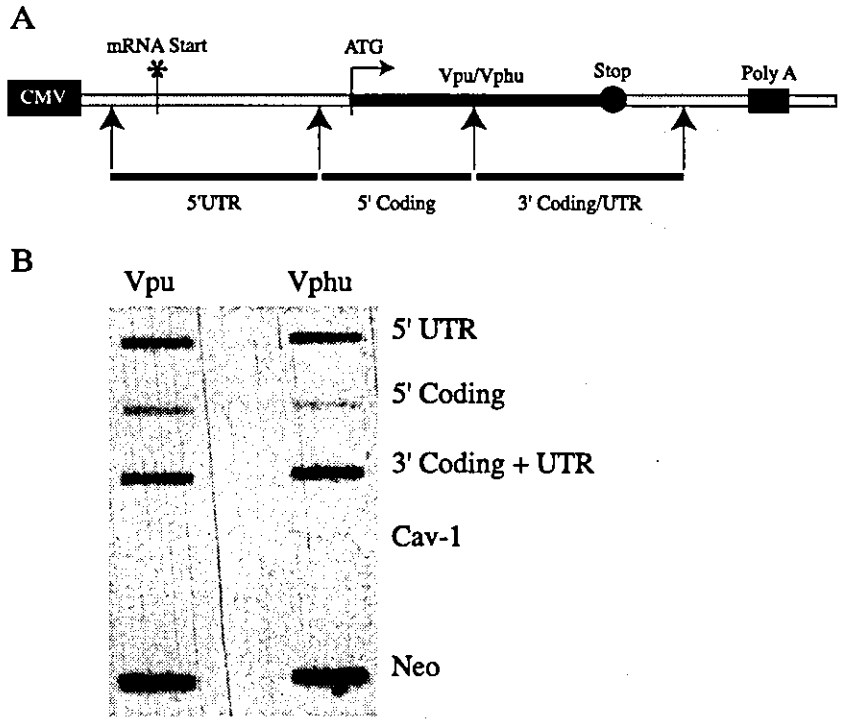

Fig. 5. Transcriptional rate of wild-type and codon-optimized *vpu* genes. (A) Schematic representation of the three cDNA probes used to detect the *vpu* and *vphu* mRNAs. (B) 293T cells were transfected with 2 μg of pcDNA-Vpu and pcDNA-Vphu and 24 h later nuclei were isolated and used in nuclear run-on assays. Nuclei were ^{32}P-labeled in vitro and hybridized to nylon membranes blotted with cDNA fragments diagramed in A. cDNA from an unrelated cellular gene (*caveolin-1*) was used as a control for specificity, and a probe for the neomycin resistance gene was used for transfection and loading controls.

neomycin resistance (*neo*) gene, present in both the pcDNA-Vpu and pcDNA-Vphu constructs served as an internal control for transfection efficiency. Cells were transfected with pcDNA-Vpu or pcDNAVphu, nuclei were isolated, and NROs were performed as described in Materials and methods. Nylon membranes were blotted with the various probes described in Fig. 5A and hybridized with 100,000 cpm of radiolabeled RNA from the NRO reactions. An unrelated cellular gene cDNA (*caveolin-1*) was used as a control for specificity and a probe for the *neo* gene was used for transfection and loading controls. As shown in Fig. 5B, RNA encoding the non-optimized Vpu was readily detectable, in contrast to the situation observed with steady-state Northern blots (see Fig. 4). In addition, all the intermediates of the full-length *vpu* mRNA, from the 5′ to the 3′ UTRs, were detected, indicating proper initiation and elongation of the non-optimized message (Fig. 5B, Vpu). Similar results were obtained when a probe spanning the complete coding region for these genes were used (data not shown). Results of the NRO also indicated that codon optimization of the *vpu* ORF did not lead to a detectable improvement in the rate of initiation or elongation of the *vphu* message (Fig. 5B, Vphu). The variations in relative intensity between probes for the same gene product are likely due to differences in affinity between the probes rather than a direct measure of the abundance of the different species of RNA. Taken together, these data show that the higher steady-state levels of *vphu* RNA observed after codon optimization are not due to enhanced transcriptional initiation or elongation.

Codon optimization increases the nuclear stability of the Vpu mRNA

Results from the NRO experiments showed that neither the initiation nor the elongation of the *vpu* RNA were affected by codon optimization. Therefore, our inability to detect steady-state levels of *vpu* RNA is likely due to nuclear or translation-coupled degradation of the mRNA. To differentiate between these two possibilities, we performed Northern blot analysis of the *vpu* and *vphu* RNA in cellular RNA fractions using a full-length probe spanning the entire transcribed RNA to detect degradation products. In the case of *vphu*, a discrete band corresponding to the full-length mRNA was detected in both the nuclear (Fig. 6, Vphu, N) and cytoplasmic fractions (Fig. 6, Vphu, C). In addition, a large proportion of the *vphu* RNA was isolated from the cytoplasmic fraction, indicating efficient nuclear export. In sharp contrast, no discrete band corresponding to full-length *vpu* RNA was detected in the nuclear or cytoplasmic fractions (Fig. 6, Vpu). Instead, a smear corresponding to products in various stages of degradation was detected in the nuclear fraction (Fig. 6, Vpu, N). Moreover, the smear was absent in the cytoplasmic fraction, indicating that the bulk of the degradation occurred in the nucleus and that no full-length or partial *vpu* RNA was exported to the cytoplasm

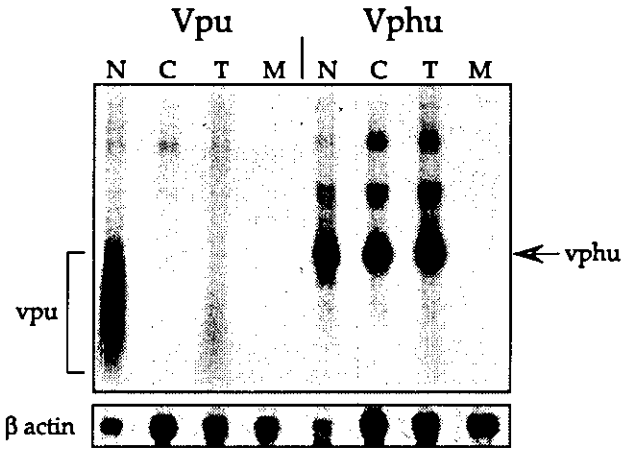

Fig. 6. Subcellular distribution of steady-state levels of *vpu* and *vphu* mRNA. 293T cells were transfected with 2 μg of pcDNA-Vpu and pcDNA-Vphu and 24 h later total RNA was extracted from nuclear (N) and cytoplasmic (C) fractions or unfractionated cells (T) and analyzed by Northern blotting with ^{32}P-labeled Vpu and Vphu cDNA probes. RNA from mock-transfected cells (M) and β-actin were used as a control for specificity and loading, respectively.

(Fig. 6, Vpu, C). These shorter *vpu* mRNA products could account for the signal detected in the NRO experiments of pcDNA-*vpu* transfected cells. Also, longer forms of *vphu* mRNA and a small amount of *vpu* mRNA were detected in the cytoplasmic fractions. These products could represent read-through of the poly A signal in pcDNA3. Taken together, these data allow us to conclude that non-optimized *vpu* fails to express Vpu protein in the absence of Rev because of a lack of cytoplasmic export as well as nuclear degradation of its mRNA. Codon optimization relieves this block by stabilizing the RNA in the nucleus and allowing its efficient export to the cytoplasm.

The codon-optimized vphu message uses a CRM1-independent nuclear export pathway

One possible explanation for the nuclear instability of the non-optimized *vpu* mRNA is that the RNA is not efficiently exported from the nucleus where its prolonged presence leads to enhanced degradation. The ability of the codon-optimized *vpu* message to utilize a different nuclear export pathway would explain the results presented in Fig. 6 and provide a mechanistic explanation for the drastic effect of codon optimization on Vpu expression. It has been reported that Rev-dependent HIV-1 mRNAs such as the *gag* mRNA use the CRM1 Ran-GTP nuclear export pathway and that inhibiting CRM1 function with the drug leptomycin B (LMB) has a pronounced negative effect on the nuclear export of Rev-dependent HIV RNA (Graf et al., 2000; Wolff et al., 1997). We therefore examined the effect of LMB treatment on the rate of Vpu synthesis. Vpu was expressed from its native ORF in a Rev-dependent context from the pNL-A1 construct. The pNL-A1 plasmid also expresses the *env* gene, providing an internal control for another Rev-dependent message. Vphu was expressed from pcDNA-Vphu in the absence of Rev. Twenty-four hours posttransfection, cells were divided into three identical aliquots and pretreated with 0, 10, or 25 nM LMB at 37°C for 2 h. Cells

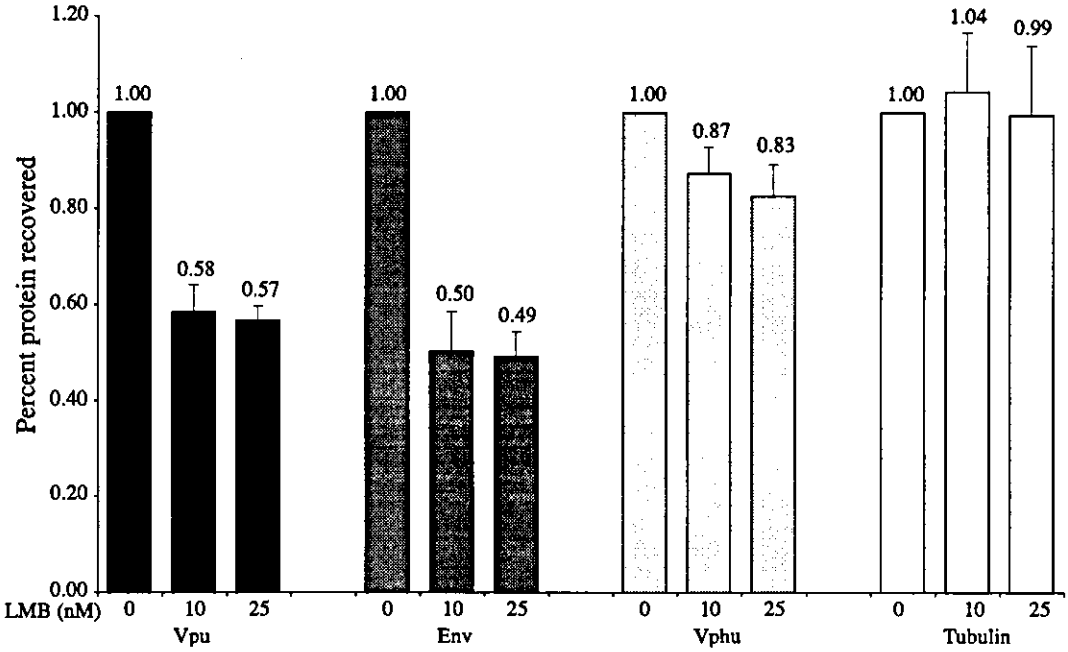

Fig. 7. Effect of LMB treatment on Vpu synthesis. HeLa cells were transfected with 9 μg pNL-A1 (Env and Vpu) or 3 μg pcDNA-Vphu (Vphu). Cells were divided into three equal aliquots and incubated with 0, 10, or 25 nM LMB for 2 h at 37°C. Cells were labeled with [^{35}S]-methionine for 1.5 h at 37°C in the presence or absence of LMB. Cell lysates were immunoprecipitated with antibodies against Vpu, Env, or tubulin, separated by SDS-PAGE, and visualized by fluorography. Bands were quantified and plotted as the ratio of LMB-treated versus untreated control.

were then metabolically labeled for 90 min with [^{35}S]-methionine in the presence or absence of the indicated amounts of LMB. Cell lysates were immunoprecipitated with antibodies to Vpu, Env, or tubulin, separated by SDS-PAGE, and visualized by fluorography (not shown). Bands were quantified with a Bio-Image analyzer and plotted as shown in Fig. 7. As expected, LMB treatment had a significant negative effect on the synthesis of the Rev-dependent Env protein, leading to a 50% reduction in Env protein synthesis during the 90-min labeling (Fig. 7, Env). A similar decrease was observed for Vpu when produced in the context of the pNL-A1 plasmid bearing the native *vpu* ORF (Fig. 7, Vpu). In contrast, LMB had little effect on the synthesis of Vpu when expressed from the codon-optimized pcDNA-Vphu plasmid, even at the highest LMB concentration used (Fig. 7, Vphu). As an internal control, we also examined the synthesis of the cellular tubulin gene both in cells transfected with either pNL-A1 or pcDNA-Vphu. As shown in Fig. 7, tubulin synthesis was unaffected by the presence of LMB, further demonstrating that the effect of the drug was specific for CRM1-dependent RNAs and not the result of general toxicity (Fig. 7, Tubulin). These data indicate that codon optimization of the *vpu* gene led to an increase in RNA stability and accelerated nuclear export by allowing the *vphu* mRNA to utilize a CRM1-independent nuclear export pathway.

Discussion

This work presents the first example of codon optimization of small HIV-1 accessory genes. We demonstrated that partial or complete codon optimization of the *vpu* and *vif* ORFs led to a dramatic enhancement of protein synthesis in the absence of the viral regulatory proteins Tat and Rev and that this was attributable to higher levels of translatable mRNA in the cytoplasm. In the case of the native *vpu* gene, we further demonstrated that the lack of protein synthesis was due to nuclear retention and degradation of its mRNA. In contrast, the mRNA produced by the codon-optimized gene was stable and efficiently exported to the cytoplasm. One important question that remains to be addressed is whether the native *vpu* message is intrinsically unstable due to the presence of destabilizing sequences or whether degradation is a consequence of the prolonged presence of the RNA in the nucleus. Our experiment using the CRM1 blocker LMB favors the latter hypothesis. Indeed, we showed that, in contrast to the native message, the codon-optimized *vpu* RNA was insensitive to LMB, suggesting a mechanism by which codon optimization relieved a nuclear export block. However, it is also possible that destabilizing sequences were still present in the codon-optimized message but that access to a new nuclear export pathway allowed the RNA to exit the nucleus before a functional degradation complex could be formed. Our codon-optimized constructs should provide ideal tools to study these questions in more details and gain new insight into the mechanisms of Rev-regulated nuclear export and RNA stability. Indeed, the small size of the *vpu* ORF will make it easier than in the case of *gag*, *pol*, or *env* to map RNA sequences involved in nuclear retention and/or RNA degradation.

Among the factors that contribute to RNA instability, a strong emphasis has been placed on the overall AU content of the message and the presence of discrete destabilizing sequences such as AREs (Hollams et al., 2002). AREs vary in size and sequence but often contain AUUUA repeats in or near AU-rich sequences. ARE sequences provide binding sites for a variety of RNA binding proteins that can affect all stages of the RNA life cycle, from transcription to nuclear export to degradation (Hollams et al., 2002). In the case of the HIV-1 *gag* message, a number of factors have been implicated in the poor expression of Gag proteins in the absence of Rev and to account for the enhanced expression following codon optimization. Most prominent among those are the inactivation of discrete INS or the decrease in the overall AU content across the length of the coding sequence (Graf et al., 2000; zur Megede et al., 2000). Yet, it is unlikely that these factors explain our results with *vpu* mRNA because no INS motifs have been defined in *vpu* and no ARE sequences conforming to the AUUUA consensus exist in *vpu*. However, the strategy employed here for the codon optimization of *vpu* resulted in a significant decrease in the AU content of the *vpu* ORF; from 63% for the wild type to 42% for the synthetic *vphu*. Interestingly, a CD4-Vpu chimera, CD4U, which we previously found to express Vpu in a Rev-independent manner when fused to the CD4 ectodomain (Bour et al., 2001), had an AU content of 49%. These data suggest that it may be the overall AU content of an mRNA rather than the presence of defined destabilizing sequence elements in the *vpu* ORF such as ARE that can confer instability to otherwise stable messages. These results further suggest that a threshold of AU content might be key to the ability of a given RNA to avoid nuclear degradation. Alternatively, it is possible that sequences near the 5′ end of a message are the main determinants of RNA stability and that introducing stabilizing CD4 sequences at the 5′ of the *vpu* coding sequence was sufficient to abrogate the negative influence of the *vpu* ORF on RNA stability. While this may be in contrast with the finding that most ARE sequences are located in the 3′ UTR of unstable mRNAs, there is experimental evidence that optimization of the first few codons on the 5′ end of poorly expressed genes contributes the most to the increased protein expression (Humphreys et al., 2000; Kim et al., 1997; Vervoort et al., 2000). The importance of 5′ sequences on RNA stability is further illustrated by our finding that partially optimizing the 5′ end of the *vif* gene was sufficient to stabilize its mRNA and enhance protein production.

Codon-optimized *gag–pol* genes have been used for the construction of lentiviral vectors that can transduce a variety of cell types. In addition to enhanced expression, the optimized synthetic genes offer a higher level of safety from